PB85-193266

Experimental Study of Flow and Dispersion in the Wakes of Three-Dimensional Low Hills

North Carolina State Univ. at Raleigh

Prepared for

Environmental Protection Agency
Research Triangle Park, NC

1985

U.S. Department of Commerce
National Technical Information Service
NTIS

PB85-193266

EPA/600/D-85/094
1985

AN EXPERIMENTAL STUDY OF FLOW AND DISPERSION IN THE WAKES OF THREE-DIMENSIONAL LOW HILLS

by

S.P.S. Arya and P.S. Gadiyaram
Department of Marine, Earth and Atmospheric Sciences
North Carolina State University, Raleigh, NC 27695, U.S.A.

Coop. Agmt. CR-807854

Project Officer

William H. Snyder
Meteorology and Assessment Division
Atmospheric Sciences Research Laboratory
U.S. Environmental Protection Agency
Research Triangle Park, NC 27711

ATMOSPHERIC SCIENCES RESEARCH LABORATORY
OFFICE OF RESEARCH AND DEVELOPMENT
U.S. ENVIRONMENTAL PROTECTION AGENCY
RESEARCH TRIANGLE PARK, NC 27711

REPRODUCED BY
NATIONAL TECHNICAL
INFORMATION SERVICE
U.S. DEPARTMENT OF COMMERCE
SPRINGFIELD, VA. 22161

TECHNICAL REPORT DATA
(Please read Instructions on the reverse before completing)

1. REPORT NO.	2.	3. RECIPIENT'S ACCESSION NO.
EPA/600/D-85/094		

4. TITLE AND SUBTITLE
AN EXPERIMENTAL STUDY OF FLOW AND DISPERSION IN THE WAKES OF THREE-DIMENSIONAL LOW HILLS

5. REPORT DATE
1985

6. PERFORMING ORGANIZATION CODE

7. AUTHOR(S)
S.P.S. Arya and P.S. Gadiyaram

8. PERFORMING ORGANIZATION REPORT NO.

9. PERFORMING ORGANIZATION NAME AND ADDRESS
Department of Marine, Earth and Atmospheric Sciences*
North Carolina State University
Raleigh, NC 27605

10. PROGRAM ELEMENT NO.
CDTA1D/02-0715 FY-85

11. CONTRACT/GRANT NO.
COOP. AGMT. NO. CR-807854

12. SPONSORING AGENCY NAME AND ADDRESS
Atmospheric Sciences Research Laboratory - RTP, NC
Office of Research and Development
U.S. Environmental Protection Agency
Research Triangle Park, NC 27711

13. TYPE OF REPORT AND PERIOD COVERED

14. SPONSORING AGENCY CODE
EPA/600/09

15. SUPPLEMENTARY NOTES
*Work conducted at the Fluid Modeling Facility of the U.S. Environmental Protection Agency, RTP, NC.

16. ABSTRACT
The EPA Meteorological Wind Tunnel was used to simulate a rural atmospheric boundary layer. Experiments were conducted on flow and dispersion over three-dimen-sional, conical hills of two different slopes (26.5^0 and 17.5^0) whose heights were 1/3 of the boundary layer depth. These measurements were made both in undisturbed and disturbed (in presence of hill) flows, using hot-wire anemometers and hydrocarbon analyzers. Most of the data were taken on the lee sides of the hills, extending to a distance of 25 hills heights (H = 235 mm). Velocity measurements over the steeper hill showed a well-defined recirculation zone, whereas no such region could be detected behind the hill of gentler slope. A trailing vortex pair in the lower part (0.35H) was indicated by the velocity profiles behind the steeper hill up to a distance of 15H. However, flow behind these hills was significantly altered up to 25H downstream. The presence of the hills caused significant changes in ground level concentrations (glc). A 50% reduction in maximum glc was observed when a point source was placed at the hilltop. A marked increase in maximum glc was observed when the source was moved to the downwind base of the hill. Enhanced vertical and lateral dispersion were evident in the immediate wake region of the hill. This phenomenon reflects the increased turbulence levels in the wake. The results of this study clearly illustrate that the slope of a conical hill is a most important parameter; it determines the location of flow separation, the size of the cavity region, and the characteristics of the wake flow dispersion.

17. KEY WORDS AND DOCUMENT ANALYSIS

a. DESCRIPTORS	b. IDENTIFIERS/OPEN ENDED TERMS	c. COSATI Field/Group

18. DISTRIBUTION STATEMENT	19. SECURITY CLASS *(This Report)*	21. NO. OF PAGES
RELEASE TO PUBLIC	UNCLASSIFIED	48
	20. SECURITY CLASS *(This page)*	22. PRICE
	UNCLASSIFIED	

EPA Form 2220-1 (Rev. 4-77) PREVIOUS EDITION IS OBSOLETE

NOTICE

This document has been reviewed in accordance with U.S. Environmental Protection Agency policy and approved for publication. Mention of trade names or commercial products does not constitute endorsement or recommendation for use.

AN EXPERIMENTAL STUDY OF FLOW AND DISPERSION IN THE WAKES OF THREE-DIMENSIONAL LOW HILLS

by

S.P.S. Arya and P.S. Gadiyaram[1]
Department of Marine, Earth and Atmospheric Sciences
North Carolina State University, Raleigh, NC 27695, U.S.A.

Abstract: The effect of three-dimensional, axisymmetric, hills on the mean flow and turbulence structure of a boundary layer is investigated through experiments conducted in a large meteorological wind tunnel. Two conical hills having slopes of 26.5° and 17.5°, and height (H) about 1/4 of the simulated boundary layer thickness were considered. Measurements of mean and turbulent flow and diffusion on the lee sides of the hills are presented and compared with the observations made without the hills. Velocity measurements behind the steeper hill (26.5°) showed a well defined recirculating zone and the presence of weak trailing vortices in the lower region (z = 0.3H), whereas no such features could be detected behind the gentler hill.

Perturbations in mean velocity, Reynolds stress and variances of velocity fluctuations in the far wake (beyond 4H) are found to decay with the downwind distance from the center of the hill according to some power laws. The decay rates of mean velocity deficit and turbulence perturbations in the far wake are compared with the theoretical predictions of Lemberg (1973) and Hunt (1974), as well as with the results of other experiments.

[1] Present address: Department of Mathematics and Physics, Southside Virginia Community College, Keysville, VA 23947, U.S.A.

Comparisons of diffusion measurements at various distances from a point source with and without the hill bring out several interesting aspects of dispersion in the wake of the gentler hill. A 40 to 65% reduction in maximum ground-level concentration (glc) was observed when the source was placed at the top of the hill, whereas a marked increase (up to six times) in the glc was noticed when the source was moved to the downwind base of the hill. Enhanced vertical and lateral dispersion was also evident in the wake region.

1. INTRODUCTION

Any surface obstacle such as a hill or a building disturbs the flow around it, typically over a distance of the order of or larger than the obstacle height or its largest dimension in the direction of flow, depending on the aspect ratio of the obstacle. Dispersion from a surface or elevated source in the disturbed boundary layer and wake of such an obstacle is expected to differ considerably from that in an undisturbed boundary layer over a flat and homogeneous surface.

Some of the distinguishing characteristics of flow and dispersion around hills and buildings have been known for sometime, at least qualitatively (for a historical perspective and literature review, see Hosker, 1984). However, detailed quantitative information on these characteristics is generally lacking, except for certain simple flow situations in the laboratory setting (in wind tunnels, water channels, towing tanks, etc). Some field studies of flow and dispersion over isolated hills have been conducted in recent years (Bradley, 1980; Jenkins et al., 1984; Strimaitis et al., 1983, Ryan et al., 1984). But measurements of flow and dispersion in these experiments have been restricted to the ground and comparatively low levels on the hills. To our knowledge, no systematic field study of flow and dispersion in the wake of an isolated hill have been made so far. Our present understanding of the obstacle wakes is largely due to laboratory experiments and theoretical or numerical model studies.

A large number of wind tunnel studies have been reported on wakes behind model fences and block buildings (Hosker, 1984). Comparatively fewer investigations have been made of the wakes of three-dimensional low hills which are completely immersed in a turbulent boundary layer. Snyder and Britter (1979) conducted some experiments on dispersion over and around steep three-dimensional hills of different aspect ratios from sources located upwind

of the hills. Castro and Snyder (1982) have reported the results of these and additional data they collected on flow field in the recirculating cavity and near-wake regions in the lee of the hills, as well as on dispersion of a nonbuoyant tracer from sources located in those regions. In the present study, the measurements were extended to the far-wake region for which simple theoretical models have been proposed. For this we used conical hills of different slopes (0.5 and 0.3) and of the same roughness as the surrounding flat terrain. The main objective was to study the structure of the far wake (beyond four hill heights) and its dispersion characteristics and to determine the possible effects of hill slope on the same. The observations are also used to test the results of the proposed theoretical models of three-dimensional wakes, as well as their underlying assumptions.

2. EXPERIMENTAL SETUP

The experiments were conducted in the EPA Meteorological Wind Tunnel, which has a 3.7m wide, 2.7m high and 18.3m long test section and is described in detail by Snyder (1979). A neutral boundary layer was developed using a 152mm fence at the entrance to the test section followed by an artificially roughened tunnel floor.

Velocity measurements were made with Thermo System Inc.'s constant temperature hot-wire anemometers. The hot-wire probes used in the x-configuration were made of a platinum-coated tungsten wire of 4 μm diameter and 1.25mm length. These were calibrated against a Pitot tube in the free stream at the beginning and end of an experimental day. The mean velocity ($\overline{U}$) and variances and covariances of fluctuating velocity components, particularly $\overline{u'^2}$, $\overline{w'^2}$, and $-\overline{u'w'}$, were determined from the usual manipulation of voltage outputs from the two cross wires. An empirical correction procedure was used to account for the small departures of the yaw response of the hot wire from

the consine law at low wind speeds. A sampling rate of 300 Hz and a sampling (averaging) time of 120s were used in all of our hot-wire measurements.

A pulsed-wire anemometer was used for identifying any recirculating or reverse flow region on the lee side of the hill. The measurement and calibration procedures used with the pulsed-wire anemometer have been discussed by Bradbury and Castro (1971) and Castro and Snyder (1982).

In our diffusion measurements, ethylene was used as a tracer gas and the same source, sampling and detecting apparatus were used as by Castro and Snyder (1982) and Pendergrass and Arya (1984b). The reader may also refer to these papers for necessary details of measurements and calibration procedures, as well as of the data acquisition system.

Two conical hills of the same height (H = 235mm) and the same roughness as the tunnel floor were used. The steeper hill had a base radius of 470mm and the side slope of 0.5 and will be referred to as hill #1. The gentler hill with a slope of 0.3 is called hill #2. Each of the model hills was placed at the center of the test section where the boundary layer was considered fully developed. The wind tunnel ceiling was adjusted to minimize the blockage effects due to the hill's presence.

3. THE FLOW FIELD

3.1 The Undisturbed boundary layer

The structure of the undisturbed boundary layer developed along the floor of the EPA meteorological wind tunnel has been described earlier by Arya and Shipman (1981), Castro and Snyder (1982), and Pendergrass and Arya (1984a) for several different surface roughnesses. In the last study the same fine Sanspray roughness (z_o = 0.07mm) and castellated fence were used as in the present study, but 900mm high vortex generators were also used to thicken the boundary layer in the former. The calibration and analysis procedures used in

computing the velocity variances and covariances from hot-wire signals were also quite different in the two studies. Consequently, there are some differences in the measured variances and covariances in the undisturbed boundary layer in these studies.

The mean velocity profiles follow the well known logarithmic law $\overline{U}/u_* = k^{-1} \ln (z/zo)$, in the surface layer ($z < 0.2\ \delta$, where δ is the boundary layer thickness), and the power law $\overline{U}/\overline{U}_\infty = (z/\delta)^n$, with an exponent $n = 0.13$, through most of the boundary layer. The gradual changes in the profiles of mean velocity and turbulent quantities with distance along the centerline of the wind tunnel are largely in response to the slow growth of the boundary layer (the boundary layer thickness δ, defined as the height where $\overline{U} = 0.99\ \overline{U}_\infty$, where $\overline{U}_\infty$ is the ambient wind speed, increased from about 0.8m at X = 8m to about 1.0m at X = 16m). No significant dependence on distance could be observed when these profiles were plotted in a similarity framework using δ for the height scale and u_* for the velocity scale. The normalized profiles of the measured standard deviations of velocity fluctuations and Reynolds stress ($-\overline{u'w'}$) in the undisturbed boundary layer are shown Figure 1; these are typical of a well-developed, zero-pressure gradient flat plate boundary layer.

3.2 The disturbed boundary layer and wake due to the hill

Mean velocity and turbulence measurements were made in the hill-disturbed boundary layers and wakes of the two conical hills. Measurements were also taken at the same positions in the undisturbed boundary layer (without the hill), so that the hill's influence could be more accurately determined.

3.2.1 The hill top and near-wake region

The mean velocity profiles above the hills' crests are compared in Fig. 2 with the profile at the same position in the undisturbed boundary layer.

Here, z' represents the height above the local surface. As expected, the flow speeds up in going over the hilltop, but the speed-up factor $S = \overline{U}(z')/\overline{U}_o(z')$, where the subscript 'o' refers to the no-hill case, is larger for the gentler hill #2 and decreases rapidly with height above the hill crest. The maximum value of $S \approx 2.0$ for the hill #2 ($S \approx 1.8$ for the hill #1) may be compared with the observed values of 2.0 - 2.5 for the speed-up factor in the field (Bradley, 1980; Jenkins et al., 1981) for hills of comparable slopes, and the computed value of 2.0 by Mason and Sykes (1979) for a gentle hill with no flow separation.

In order to have an approximate idea of flow separation and recirculating or reverse flow regions, if any, some measurements were made with a dual Pitot tube and pulsed-wire anemometer on the lee side of the hill #1. Figure 3 shows the locus of zero mean velocity on the centerline of the hill; the flow reversed direction below this line. In the lateral direction, the region of reverse flow had a maximum width of about 1.6 H which occurred at a distance of 0.5H downstream of the hill crest. The dimensions of the recirculating flow region are similar to those reported by Castro and Snyder (1982) for a slightly rougher cone of the same height and slope as our steeper hill #1. Attempts were also made to identify the possible reverse flow region behind the gentler hill #2. Smoke visualizations indicated flow separation occurring at the crest, but reverse flow appeared to have occured only intermittently in a small and shallow region just behind the crest. No pulsed-wire measurements were made to identify it in the mean flow.

For a conical hill of the same slope as our hill #1, but with a slightly different roughness, Castro and Snyder (1982) have presented more pulsed wire measurements of mean velocity and longitudinal velocity variance in the cavity and near-wake regions. In particular, the $\overline{u'^2}$-profiles at different

normalized distances (x/H) behind the crest along the centerline indicate that, initially, the turbulent kinetic energy grows with distance in the wake reaching a maximum value at x/H ≈ 2, and thereafter it decays with distance. In the present study, our emphasis has been on the far-wake region (x/H > 4).

3.2.2 Far-wake region

The vertical profiles of normalized mean velocity at various positions in the wakes of the two hills are presented in Fig. 4. For comparison, the profile at the farthest location in the undisturbed (no-hill) boundary layer is also included. Note that the reduction in velocity is confined to only about 2H in the vertical, but extends to distances of more than 25H for hill #1 and 15H for hill #2.

As a result of reduced mean velocities and increased turbulence in the wake, turbulence intensities may be expected to be greatly increased due to the presence of the hill. This is clearly demonstrated by the vertical profiles of vertical turbulence intensity ($\sigma_w/\overline{U}$) along the centerline of the wake (see Fig. 5). The hill slope does not appear to have any appreciable effect on the maximum turbulence intensity, but the vertical extent of the flow with large turbulence intensities is considerably larger for the steeper hill. Similar behavior is observed for the longitudinal turbulence intensity and the Reynolds stress, whose profiles are omitted for the sake of brevity.

A few lateral profiles of mean velocity and Reynolds stress measured in the wake of the steeper hill #1 are shown in Figs. 6 and 7. The characteristic 'double-humped' shape is indicative of the influence of trailing vortices forming on the sides of the hill. Measurement of Castro and Snyder (1982) showed similar but more enhanced effect in the near-wake region of a laterally elongated 3-D hill. This pattern was observed for our conical hill #1 up to 10H downwind, especially in the lower part (z < 0.3H), but not

in the case of hill #2 which produced no flow separation on its sides.

A simple and informative way of describing the hill's influence on the flow is to examine the differences in the mean flow and turbulence quantities with and without the hill (Lemberg, 1973; Hunt, 1974, 1978). Figures 8-11 represent the profiles of the normalized perturbations in $\overline{U}$, $\overline{u'^2}$, $\overline{w'^2}$, and $\overline{u'w'}$ at various downwind distances along the centerline in the wakes of the two hills. They show that the hill-induced perturbations in the core region (around the maximum values) decay monotonically with distance behind the hill and the height corresponding to the maximum perturbation and the wake thickness increase with distance. These features are characteristic of a growing and relaxing wake and have been observed in other two- and three-dimensional wakes (Counihan et al., 1974; Arya and Shipman, 1981a; Lemberg, 1973; Hunt, 1978). In the lower part of the wake or the so-called wall layer, the perturbation in mean velocity and turbulent quantities are found to be small and frequently of different sign than those in the core of the wake. The same phenomenon has been observed and also theoretically predicted to occur in the wall layer behind two-dimensional low hills (Counihan, et al., 1974; Jackson and Hunt, 1975).

The most dramatic influence of the hill slope appears to be on the height z_{max} associated with the maximum perturbations in the wake. Figures 8-11 show that for all the perturbation quantities, z_{max} for the steeper hill #1 is much larger than that for hill #2. This may be due to the larger vertical extent of the separated flow region and the associated shear layer in which bulk of the wake turbulence is generated. The variation of z_{max} with distance gives some idea about the rate of growth of the wake. It is shown in Fig. 12 for the two hills and different perturbation quantities. There is some difference in the heights of the maximum perturbations in mean velocity and turbulent quantities, but their growth rates are similar. More importantly, the rate of

the growth, as measured by the value of the exponent γ in the fitted power-law relation

$$z_{max}/H = \beta(x/H)^{\gamma} \tag{1}$$

is smaller for the steeper hill. The variations of β and γ with the hill slope are qualitatively similar to those observed in the case of two-dimensional hills (Capuano, 1983). Our observed value of $\gamma = 0.49$ for the gentler hill with no significant flow separation is in good agreement with the theoretical predictions of the growth of three-dimensional wakes by Lemberg (1973) and Hunt (1974).

The normalized maximum perturbations in the mean velocity, velocity variances and the Reynolds stress in the wake are plotted in Figs. 13-14 as functions of the normalized distance x/H. Following the guidance of earlier experimental and theoretical studies (Lemberg, 1973; Hunt, 1974), the following power-law relations are fitted through the data in Figs. 13-14:

$$-\Delta(\overline{U})_{max}/\overline{U}(H) = m\,(x/H)^{c} \tag{2}$$

$$\Delta(\overline{u'^2})_{max}/\overline{U}^2(H) = p\,(x/H)^{d} \tag{3}$$

$$\Delta(\overline{w'^2})_{max}/\overline{U}^2(H) = q\,(x/H)^{e} \tag{4}$$

$$\Delta(\overline{-u'w'})_{max}/\overline{U}^2(H) = r\,(x/H)^{f} \tag{5}$$

The exponents and coeffecients in the above relations obtained from a least-square fitting procedure are given in Table 1 for the two hills.

Table 1: Empirical values of the coefficients and exponents in Eqs. (2) - (5) for perturbations in the wakes of the two conical hills

Hill	Slope	(2) m	(2) c	(3) p	(3) d	(4) q	(4) e	(5) r	(5) f
#1	0.5	1.50	-1.14	0.44	-1.64	0.33	-1.50	0.13	-1.60
#2	0.3	3.55	-1.53	0.32	-1.53	0.28	-1.70	0.16	-1.70

The small differences in the estimated coefficients and constants in turbulence decay relations for the two hill wakes are probably not significant, because of the limited number (7) of data points used for evaluating these constants. The exponent values ranging from -1.5 to -1.7 are significantly different, however, from the values (= -2) predicted by theoretical models of Lemberg (1973) and Hunt (1974), which are based on overly simplistic assumptions about eddy viscosity and perturbation levels in the wake. Similar types of theoretical models for two-dimensional wakes in turbulent boundary layers (Counihan, et al., 1974; Jack and Hunt, 1975) have also been shown to predict more rapid decay of perturbations in turbulent quantities with distance in comparison to observations (Arya and Shipman, 1981; Capuano, 1983). The latter (observations) indicated no difference in the exponents of decay relations for the various perturbations, each having a value of about -1. For the three-dimensional wakes studied here, it is not clear whether and why the exponent in the decay relation (2) for $-\Delta U$ might be different from the average exponent of about -1.6 in Eqs. (3)-(5) for turbulence perturbations. Consideration of the available data on mean velocity deficits in the wakes of other surface-mounted obstacles (see Fig. 15) suggests that the same value of -1.6 might be appropriate also for the exponent in Eq. (2).

4. THE CONCENTRATION FIELD

4.1 Undisturbed boundary layer

The concentration fields due to the surface and elevated point sources in the undisturbed boundary layer over homogeneous surfaces have been described by Pendergrass and Arya (1984b). Their results for the fine-Sanspray boundary layer (FBL) show that the ground-level concentration (glc) for the surface release decreases with distance x from the source in proportion to $x^{-1.5}$. For the elevated releases, the same power law describes the glc far downwind from

the location (x_{max}) of the maximum glc C_{max} (see Fig. 16) while $x_{max} \alpha H_s^{1.2}$, and $C_{max} \alpha H_s^{-1.9}$, where H_s is the stack height. A similarity plot of C/C_{max} vs. x/x_{max} in Fig. 16 collapses all of our measured glc profiles for a wide range of stack heights. Such a similarity representation was suggested by Castro and Snyder (1982) who also proposed an analytic expression for the same.

Most of the concentration data will be presented in terms of the normalized concentration

$$\chi = \frac{C \, \bar{U}_\infty \, H^2}{Q} \qquad (6)$$

Where C is the measured volumetric concentration corrected to background concentration, H is the characteristic height scale which is taken here as the hill height (H = 235mm) and Q is the source strength (the volumetric flow rate of the tracer gas) which was varied with the stack height roughly in proportion to the velocity at the stack height H_s.

The longitudinal, lateral and vertical profiles of normalized concentration χ for the surface and elevated sources in the undisturbed boundary layer are similar to those presented earlier by Pendergrass and Arya (1984b) (the reader should keep in mind, however, the differences in the scaling parameters, such as H and Q used in the two studies) and will not be repeated here, except when comparing with the concentration profiles in the presence of the hills.

4.2 Dispersion in the hill-disturbed boundary layer and wake

Since, Castro and Snyder (1982) have already reported concentration measurements in the disturbed boundary layers and wakes of several steep hills, including a conical hill of the same slope and height as our hill #1, we have restricted this investigation to only the gentler hill #2.

4.2.1 Sources on the hill top

First, we discuss the results of concentration measurements for sources located on the top of the hill (denoted here by $x_s = 1$), which may be considered as the most desirable location so far as ground level concentrations are concerned. The glc profiles along the plume centerline for different source heights located on the top of the hill #2 are shown in Fig. 17. The glc profiles for the same sources without the hill are also shown for comparison. Note that for all source heights up to 0.5H, the centerline surface concentrations, including the maximum glc, are reduced by nearly a factor of two due to the presence of the hill. This is in spite of the fact that the hill-induced turbulence in the wake diffuses the material more rapidly in both the vertical and lateral directions, as shown by the vertical and lateral concentration profiles in Figs. 18 and 19 for the ground level source ($H_s = 0$) at the hill top. The main reason for the reduction in surface concentrations from those for the no-hill case is that in the former the plume becomes elevated and detached from the surface as soon as it leaves the source at the hill top. Thus, the effect of the hill is essentially to increase the effective source height H_e, such that $H_e > H_s + H$. The relative effect of the hill on H_e and, hence, on the maximum glc, diminishes as the stack height increases and might become insignificant only for very tall stacks ($H_s >> H$). For tall stacks relative to the hill, the hill wake effects can be ignored and the effect of the hill can simply be considered by taking $H_e = H_s + H$ for a nonbuoyant release. Any plume rise due to buoyancy effects is to be considered separately in arriving at an effective source height.

4.2.2 Sources at the downwind base of the hill

In the absence of any appreciable recirculating cavity region, probably the worst location for a point source might be at the downwind base of the hill (denoted here by $x_s = 2$) where the plume is likely to be brought down to the ground level much closer to the location of the source as compared to that for the no-hill case (Arya et al., 1981; Castro and Snyder, 1982).

Figure 20 shows the longitudinal glc profiles along the plume centerline for sources located at the downwind base of the hill #2. Here the distance indicated is from the center (crest) of the hill and the source location x_s is shown by an arrow. Note that for a stack height $H_s < 0.5H$, the maximum glc is indeed located fairly close but downwind of the source, and large concentrations are also found to occur on the hill slope upwind of source. Downwind of the location of the maximum glc, concentration falls very rapidly at first and in proportion to $x^{-1.5}$ at large distances from the source which is similar to the power-law behavior in the absence of the hill. However, a comparison in Fig. 21 with the glc profiles without the hill shows that for $H_s < 0.5H$, the maximum ground level concentrations are considerably increased by the presence of the hill, but concentrations beyond a few hill heights downwind are actually reduced and become more or less independent of the source height. These hill-induced effects are expected to diminish with increasing height of the stack and may become insignificant only for very tall stacks (say, $H_s > 2H$).

The vertical concentration profiles in the far-wake region are shown in Fig. 22 and compared with those in the absence of the hill; the former show clearly the enhanced vertical diffusion due to the hill-induced turbulence. There are some interesting differences in these profiles and those of Fig. 18 for the source located at the top of the hill.

The observed concentration fields due to sources located at the downwind base of the hill #2 are qualitatively similar to those reported by Castro and Snyder (1982) for their steeper conical hill (slope = 0.5) and the sources located at the reattachment point (the downwind edge of the separated flow zone). They show that, for steep hills, the location of the source with respect to the separated 'cavity' becomes important. A terrain amplication factor A, defined as the ratio of the maximum glc in the presence of the hill to that in its absence for the same source, can be used in a gross sense to represent the influence of the hill on dispersion for different source heights and locations. Table 2 compares our estimated values of A with these obtained from other studies.

Table 2. Amplication factors for conical hills for different source heights and locations relative to the hill

Hill Slope (Reference)	Source Height (H_s/H)	Amplification Factor (A) Source Location		
		Upwind	Hill Top	Downwind
0.5 (26.5°)	0.5	3.3	-	-
(Snyder and Britter, 1979)	1.0	1.8	-	-
0.5 (26.5°)	0.5	-	-	6.0
(Castro and Snyder, 1982)	1.0	-	-	3.0
	1.5	-	-	2.1
0.3 (17.5°)	0.125	-	0.59	4.0
(Present study)	0.25	-	0.35	5.9
	0.50	-	0.45	5.6
	1.0	-	0.51	2.6

Here, only the maximum values of A from Castro and Snyder (1982) are given. The maximum values of A for the two hill slopes are comparable, and correspond to a source of height 0.25H - 0.5H, located near the downwind base of the hill.

5. CONCLUSIONS

The results of wind tunnel measurements of flow and dispersion in the wakes of conical hills of height about one-fourth of the boundary layer thickness and slopes 0.5 and 0.3 have brought out several interesting features. The observed speed-up of flow at the hill top is comparable to that observed over more rounded (flat-topped) hills in the field (Bradley, 1980; Jenkins et al., 1981). The steeper hill is characterized by the occurrence of a separated recirculating flow region in the lee of the hill extending beyond the hill base and vortex shedding from its sides. Such features are inconspicuous on the gentler hill.

The maximum perturbations in mean velocity, velocity variances and the Reynolds stress in the far wakes (beyond 4H) of both the hills decay with distance (x) from the hill roughly in proportion to $x^{-1.6}$, as the wake thickness and width grow with distance. The proportionality coefficient in the decay relations are however dependent on the hill slope and, presumably, on other factors not varied in the present study. The exponent (1.6) is significantly smaller than that predicted ($\simeq 2$) by theoretical models of Lemberg (1973) and Hunt (1974) for turbulence decay in three-dimensional wakes.

Concentration measurements are reported for sources located at the top and downwind base of the gentler hill. For the sources located on the hill top, the maximum ground level concentrations are reduced by 40 to 65% of their values for the no-hill case, due to the increase in the effective height of the source in the presence of the hill. On the other hand, the maximum surface concentrations are considerably increased (by factors of 2.6 to 5.9) for sources located at the downwind base of the hill. For the latter case, our results are similar to those reported by Castro and Snyder (1982) for a steeper (slope = 0.5) hill.

The results of this and previous studies indicate that the hill slope and the aspect ratio are probably the most important parameters in determining the flow and dispersion characteristics of the disturbed boundary layer and wake behind an isolated hill, at least in neutral flows. Further studies should be conducted on flow and dispersion around combinations of two or more low hills immersed in neutral, as well as stratified boundary layers.

Acknowledgements: We are grateful to Dr. W. H. Snyder and his staff at the EPA Fluid Modeling Facility for their help and cooperation in conducting these experiments.

This research was supported through the Cooperative Agreement CR-807854 between the U.S. Environmental Protection Agency and North Carolina State University (Dr. S.P.S. Arya, Principal Investigator). It has not been subjected to the Agency's required peer and policy review and, therefore, does not necessarily reflect the views of the Agency. No official endorsement should be inferred.

REFERENCES

Arya S.P.S. and Shipman M. S. (1981) An experimental investigation of flow and diffusion in the disturbed boundary layer over a ridge-I. Mean flow and turbulence structure. Atmospheric Environment, 15, 1173-1184.

Arya S.P.S., Shipman M. S. and Courtney L. Y. (1981) An experimental investigation of flow and diffusion in the disturbed boundary layer over a ridge-II. Diffusion from a continuous point source. Atmospheric Environment, 15, 1185-1194.

Bradbury L.J.S. and Castro I. P. (1971) A pulsed-wire technique for velocity measurements in highly turbulent flows. J. Fluid Mech., 49, 657-691.

Capuano M. E. (1983) The effect of hill slope on flow and dispersion over two-dimensional hills - A wind tunnel study. M.S. Thesis, Department of Marine, Earth and Atmospheric Sciences, North Carolina State University, Raleigh, N.C., U.S.A., 153 p.

Castro I. P. and Snyder W. H. (1982) A wind tunnel study of dispersion from sources downwind of three-dimensional hills. Atmospheric Environment, 16, 1869-1887.

Counihan J., Hunt J.C.R. and Jackson P.S. (1974) Wakes behind two-dimensional surface obstacles in turbulent boundary layers. J. Fluid Mech., 64, 529-563.

Hosker R. P. (1984) Flow and diffusion near obstacles. Chapter 7, Atmospheric Science and Power Production, D. Randerson, Editor, Technical Information Center, U.S. Department of Energy, 241-326.

Hunt J.C.R. (1974) Wakes behind buildings. ARC Report 35601, Atmos. 229, Aeronautical Research Council, London, 28 p.

Hunt J.C.R. (1978) Wind over hills. Proceedings, Workshop on the Planetary Boundary Layer, 14-18 August 1978, Boulder, Colorado, J.C. Wyngaard, editor, American Meteorological Society, 107-157.

Jackson P.S. and Hunt J.C.R. (1975) Wind flow over low hill. Quart. J. Roy. Meteor. Soc., 101, 929-955.

Jenkins G. J., Mason P. J., Moore W. H. and Sykes R. I. (1981) Measurements of flow structure around Ailsa Craig, a steep, three-dimensional isolated hill. Quart. J. Roy. Meteor. Soc., 107, 833-851.

Lemberg R. (1973) On the wakes behind bluff bodies in a turbulent boundary layer. Ph.D. Dissertation, Report No. BLWT-3-73, Boundary Layer Wind Tunnel Laboratory, University of Western Ontario, London, Ontario, Canada, 162 p.

Pendergrass W. and Arya S.P.S. (1984a) Dispersion in neutral boundary layer over a step change in surface roughness-I. Mean flow and turbulence structure. Atmospheric Environment, 18, 1267-1279.

Pendergrass W. and Arya S.P.S. (1984b) Dispersion in neutral boundary layer over a step change in surface roughness-II. Concentration profiles and dispersion parameters. Atmospheric Environment, 18, 1281-1296.

Ryan W., Lamb B. and Robinson E. (1984) An atmospheric tracer investigation of transport and diffusion around a large isolated hill. Atmospheric Environment, 18, 2003-2021.

Snyder W. H. (1979) The EPA Meteorological Wind Tunnel-Its design and operating characteristics. U.S. Environmental Protection Agency. Report No. EPA-600/4-79-051, Research Triangle Park, N.C., U.S.A.

Snyder W. H. and Britter R. E. (1979) Aspect ratio study. Data Report (unpublished), Fluid Modeling Facility, U.S. Environmental Protection Agency, Research Triangle Park, N.C., U.S.A.

Strimaitis D. G., Venkatram A., Greene B. R., Hanna S. R., Heisler S., Lavery T. F., Bass A. and Egan B. A. (1983) EPA complex terrain model development-Second Milestone Report-1982, EPA-600/3-83-015, Environmental Protection Agency, Research Triangle Park, N.C., U.S.A., 375 p.

List of Figures

Fig. 1. Normalized profiles of σ_u, σ_v, and σ_w and Reynolds stress in the simulated boundary layer at X = 10m.

Fig. 2. Velocity profiles at the tops of the hills compared with that for the undisturbed (no-hill) boundary layer.

Fig. 3. Locus of zero longitudinal-mean velocity on the centerline in the lee of hill #1.

Fig. 4. Normalized mean velocity profiles at various locations in the far-wake region: (a) hill #1; (b) hill #2.

Fig. 5. Vertical turbulence intensity profiles at various locations in the far-wake region: (a) hill #1; (b) hill #2.

Fig. 6. Lateral distribution of normalized mean velocity in the wake of hill #1.

Fig. 7. Lateral distributions of normalized Reynolds stress in the wake of hill #1.

Fig. 8. Vertical distributions of normalized mean velocity deficits in the wakes of the two hills.

Fig. 9. Vertical distributions of normalized perturbations in the longitudinal variance in the wakes of the two hills.

Fig. 10. Vertical distributions of normalized perturbations in the vertical velocity variance in the wakes of the two hills.

Fig. 11. Vertical distributions of normalized perturbations in Reynolds stress in the wakes of the two hills.

Fig. 12. Variation of the heights of maximum perturbations with distance behind the hills.

Fig. 13. Variations of the maximum in mean velocity deficit with distance behind the hills.

Fig. 14. Variations of the maxima in perturbations of velocity variances and Reynolds stress with distance: (a) hill #1; (b) hill #2.

Fig. 15. Comparison of variations of the maximum in mean velocity deficit in the wakes of the various three-dimensional obstacles.

Fig. 16. Similarity representation of longitudinal glc profiles downwind of elevated sources in the undisturbed boundary layer.

Fig. 17. Comparison of longitudinal glc profiles with and without the hill for sources located at the hill top.

Fig. 18. Comparison of vertical concentration profiles at various downwind distances from a surface source located at the hill top with those from the same source in the absence of the hill.

Fig. 19. Comparison of lateral concentration profiles due to a surface source located at the hill top with those in the absence of the hill.

Fig. 20. Longitudinal glc profiles due to the various height sources located at the downwind base of the hill.

Fig. 21. Comparison of longitudinal glc profiles with and without the hill for sources located at the downwind base of the hill.

Fig. 22. Comparison of vertical concentration profiles at various downwind distances from a ground source located at the downwind base of the hills with those in the absence of the hill.

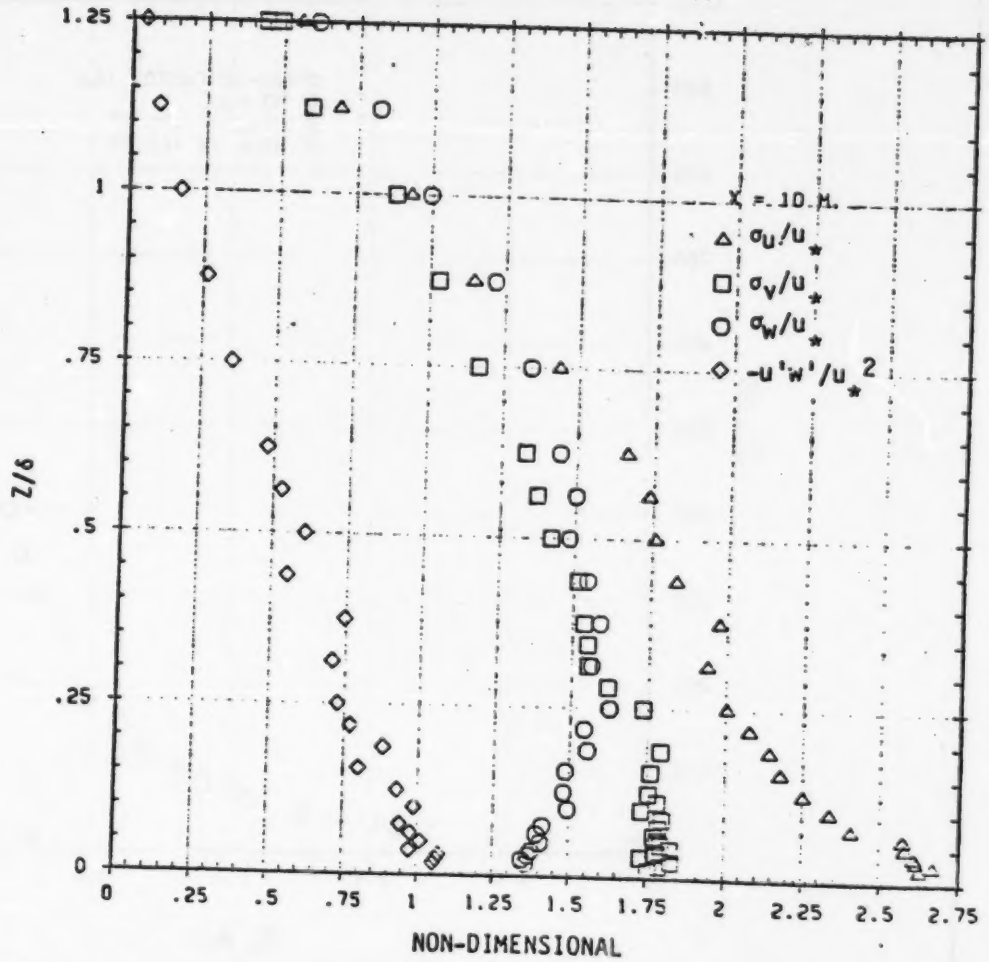

Figure 1. Normalized profiles of σ_u, σ_v, σ_w, and Reynold's stress in the simulated boundary layer at X = 10 m.

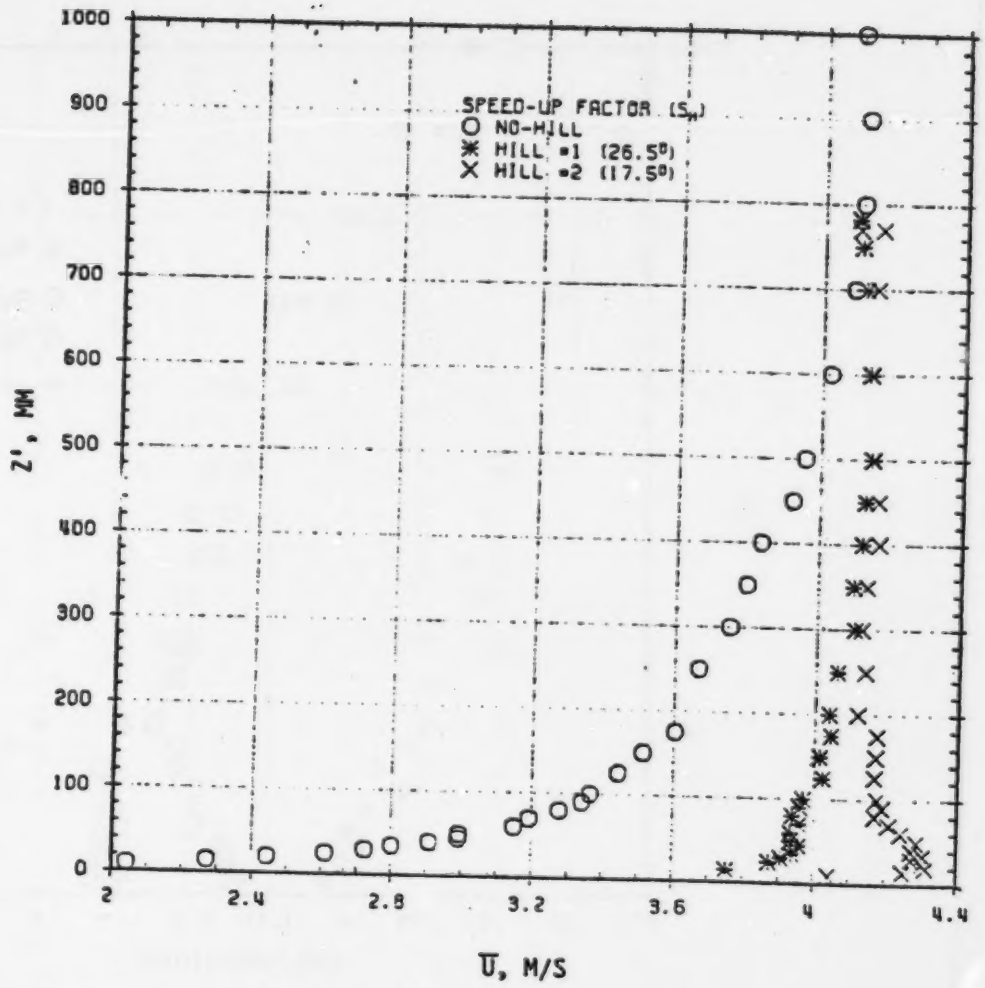

Fig. 2. Velocity profiles at the tops of the hills compared with that for the undisturbed (no-hill) boundary layer.

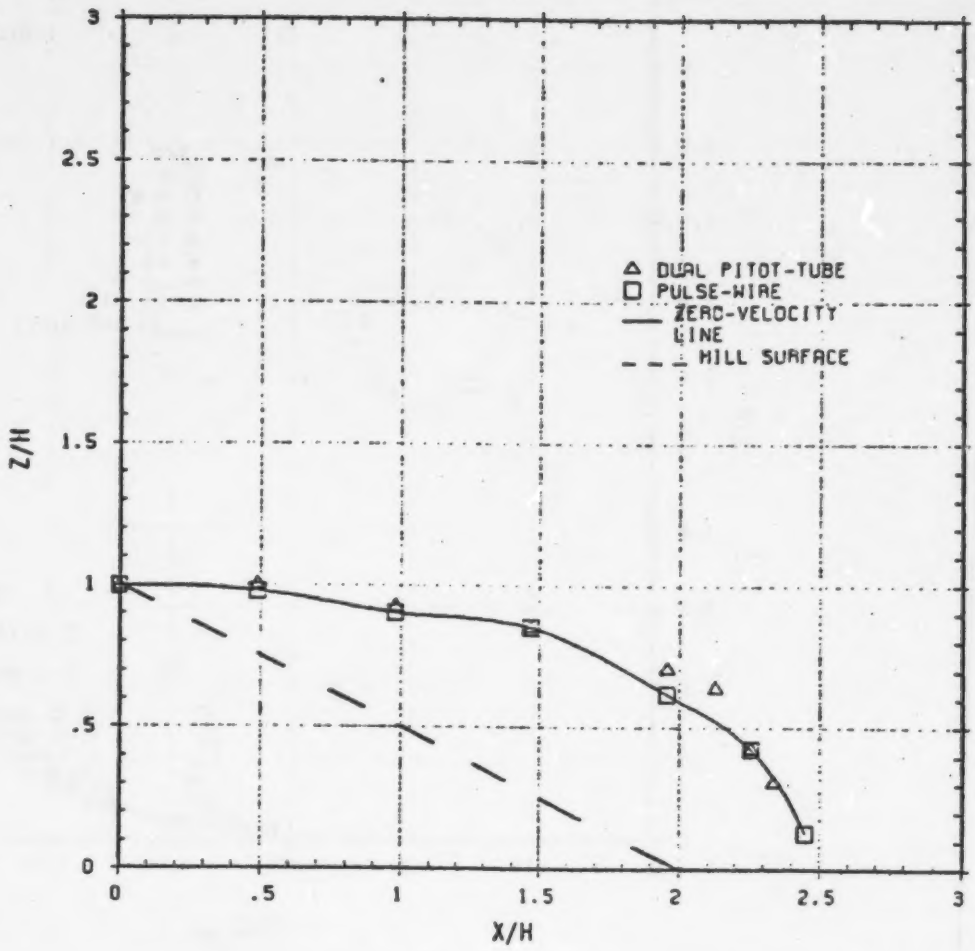

Fig. 3. Locus of zero longitudinal-mean velocity on the centerline in the lee of hill #1.

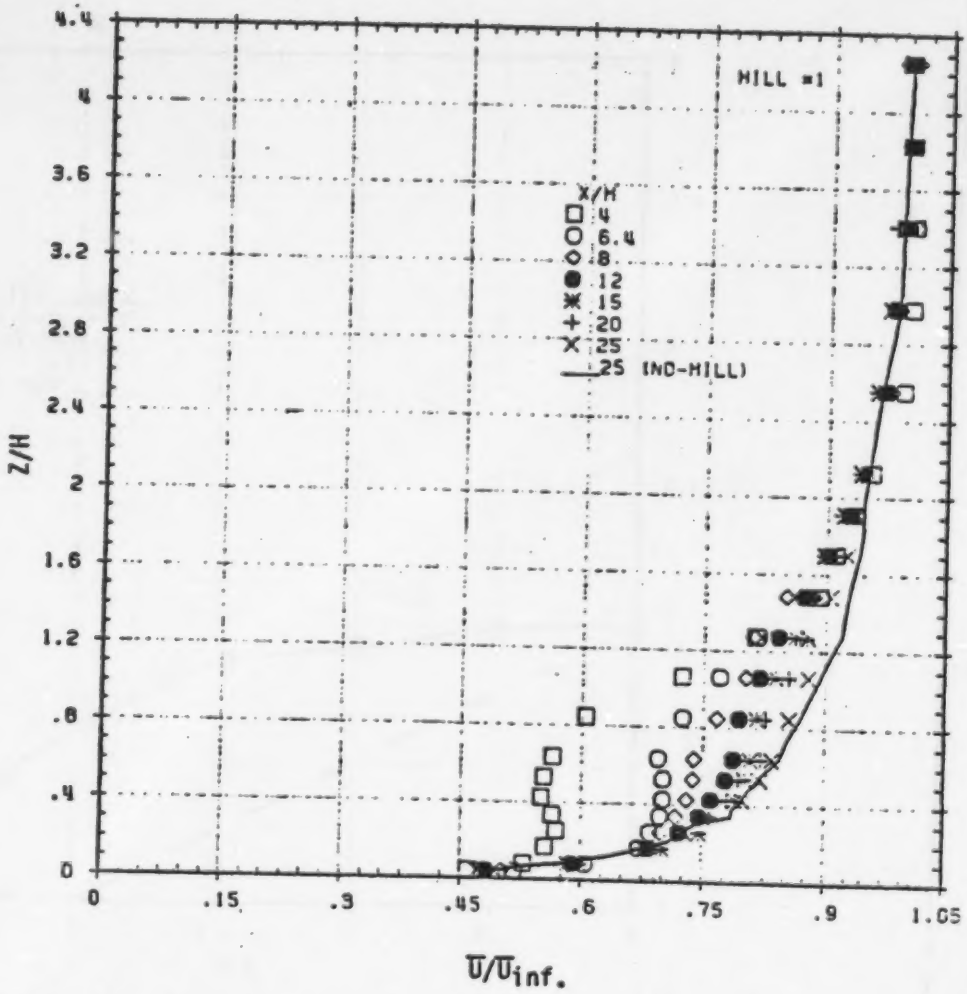

Figure 4(a). Normalized mean velocity profiles at various positions downwind of hill #1.

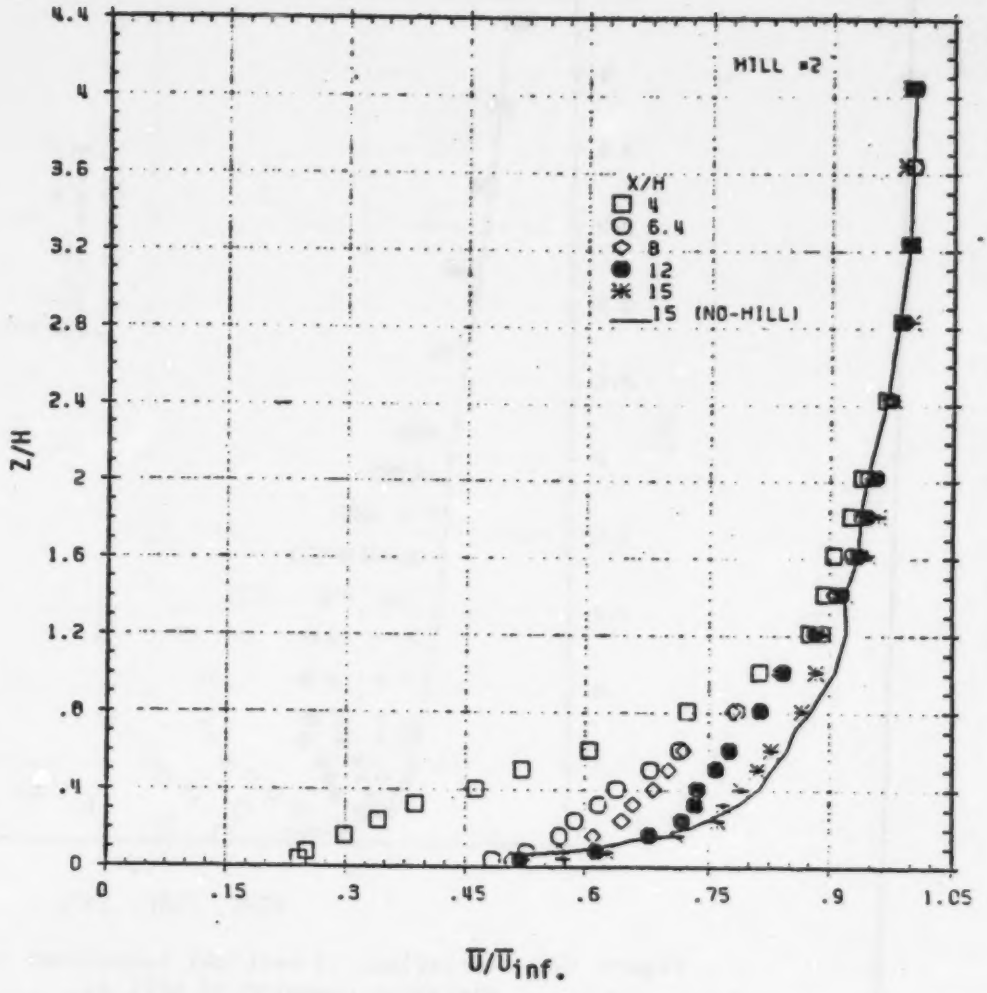

Figure 4(b). Normalized mean velocity profiles at various positions downwind of hill #2.

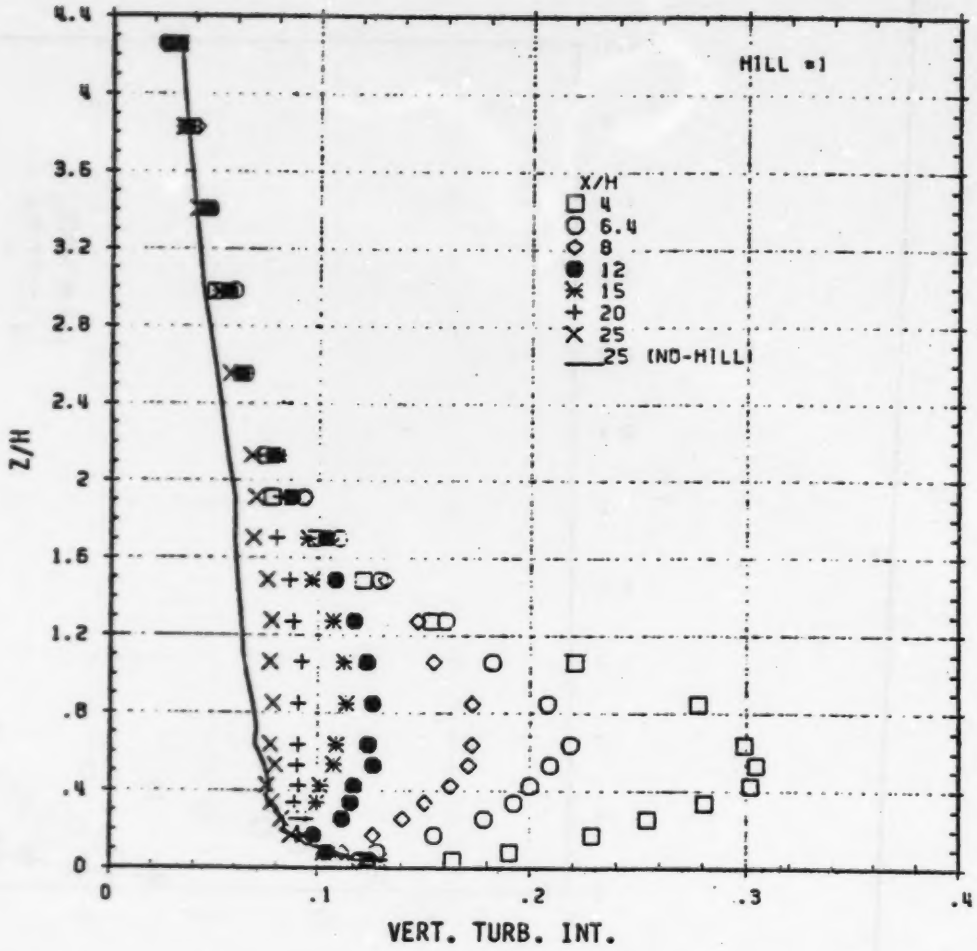

Figure 5(a). Variations in vertical turbulence intensity at various distances downwind of hill #1.

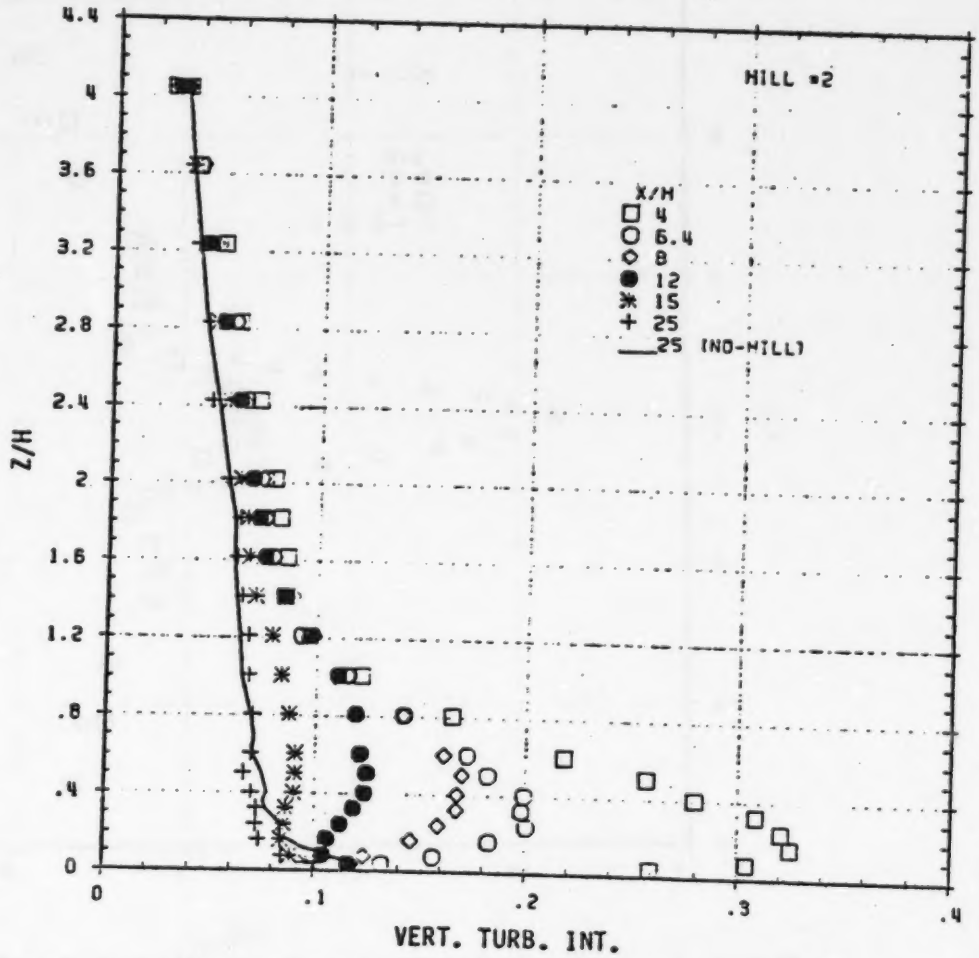

Figure 5(b). Variations in vertical turbulence intensity at various distances downwind of hill #2.

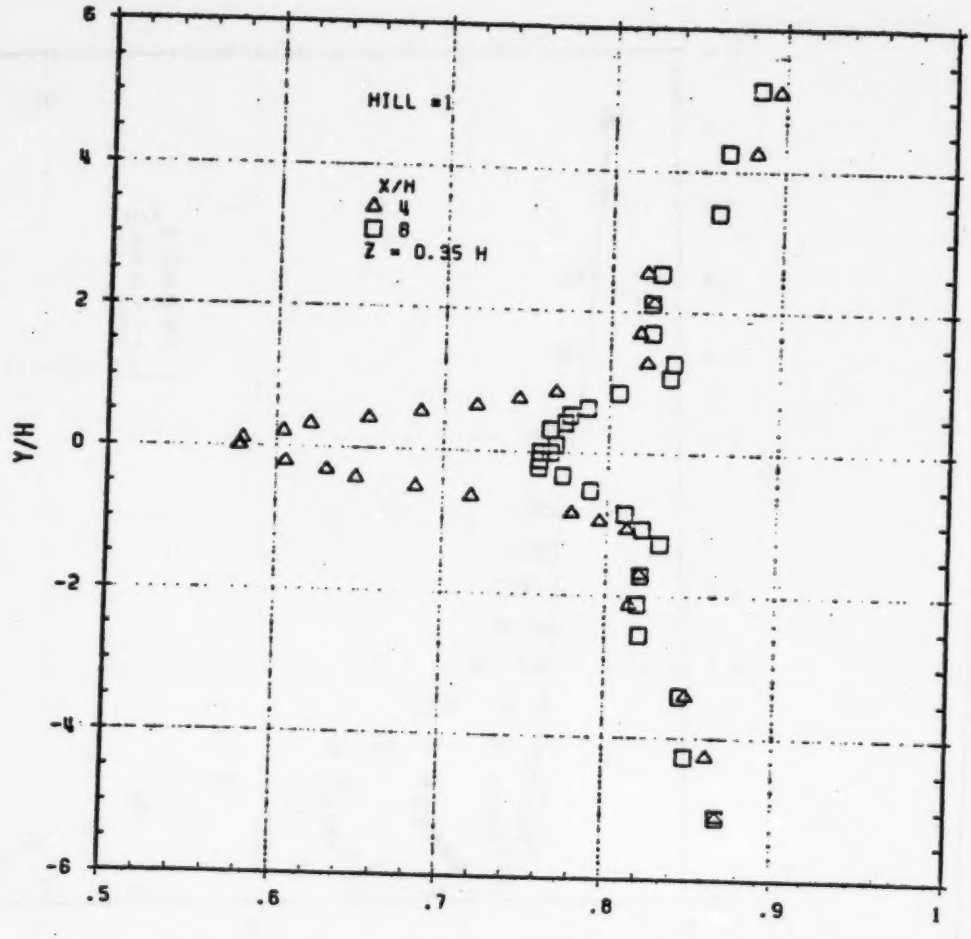

Figure 6. Lateral distribution of normalized mean velocity in the wake of hill #1.

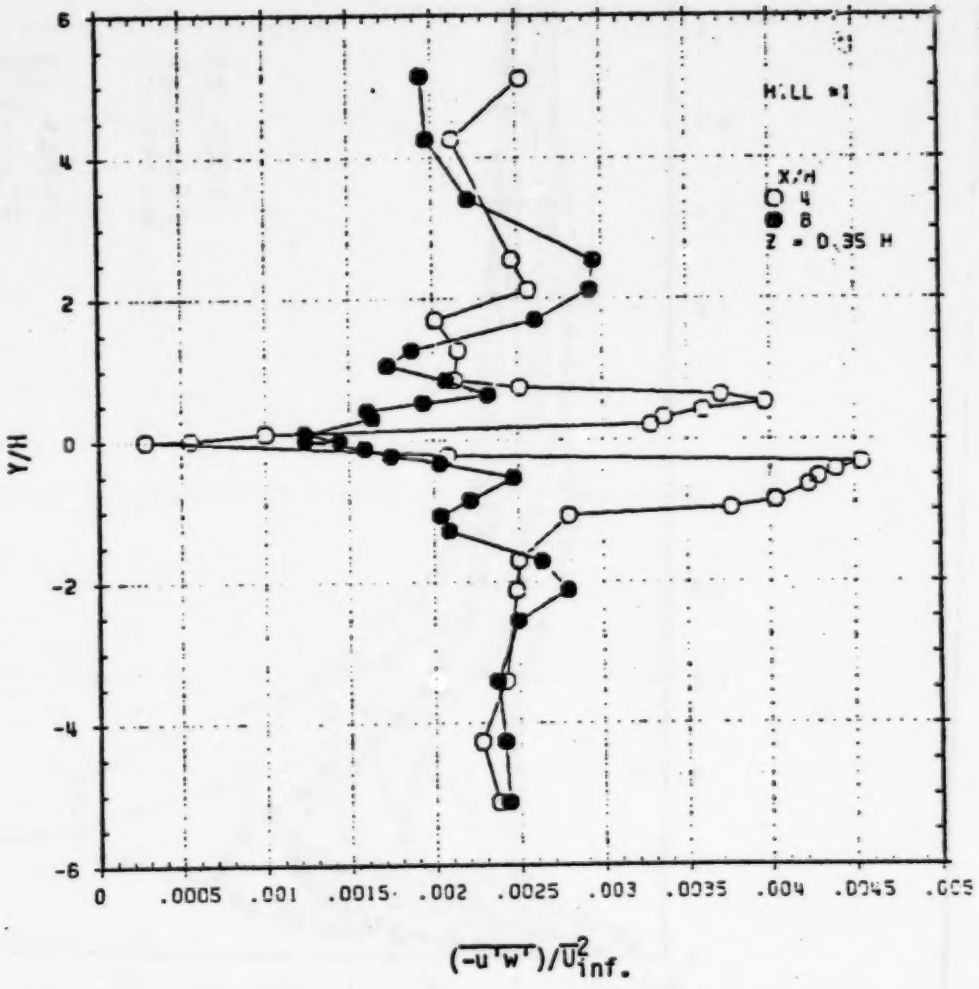

Figure 7. Lateral distribution of normalized Reynold's stress in the wake of hill #1.

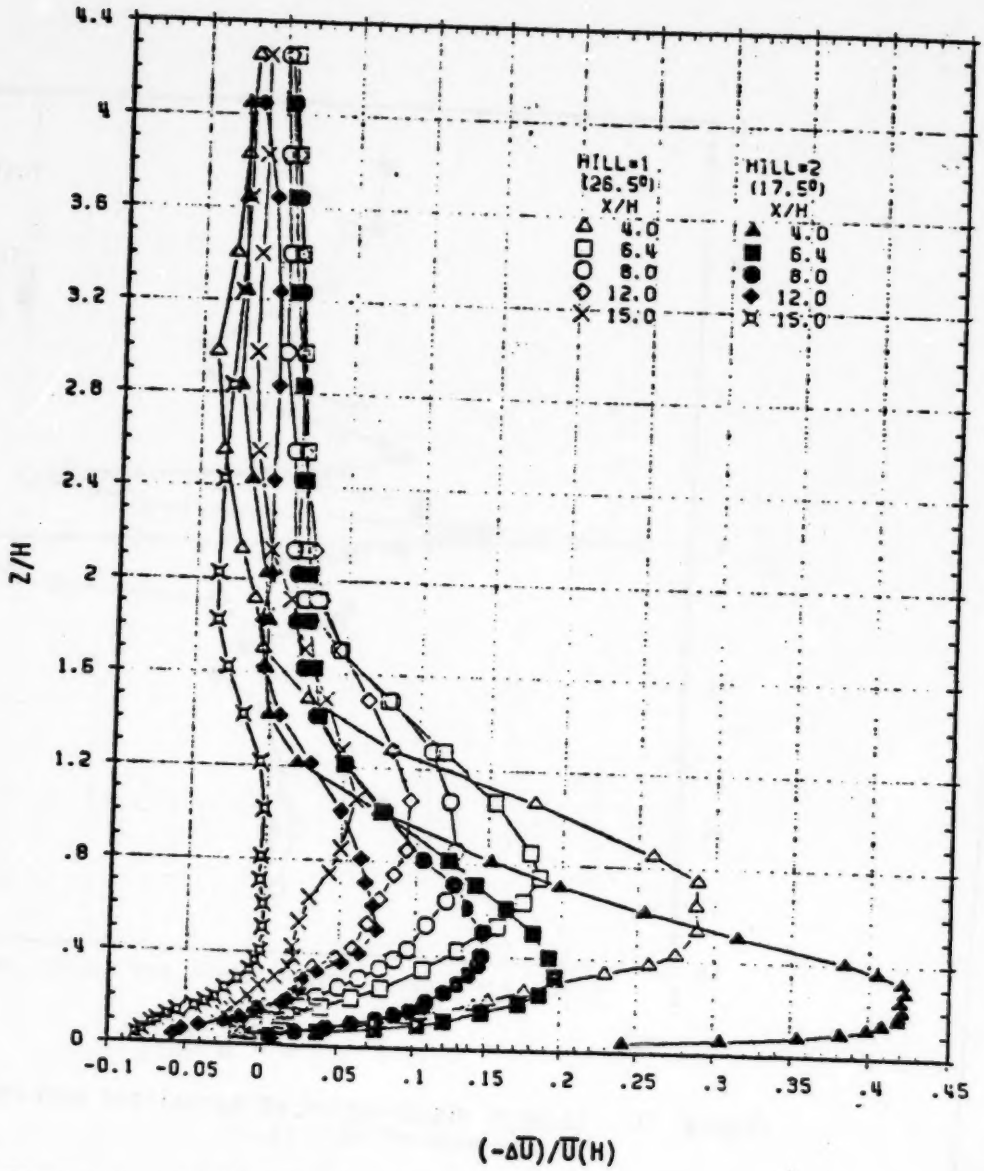

Figure 8 Distribution of mean velocity deficit ($-\overline{U}/\overline{U}(H)$) in the wakes of the hills.

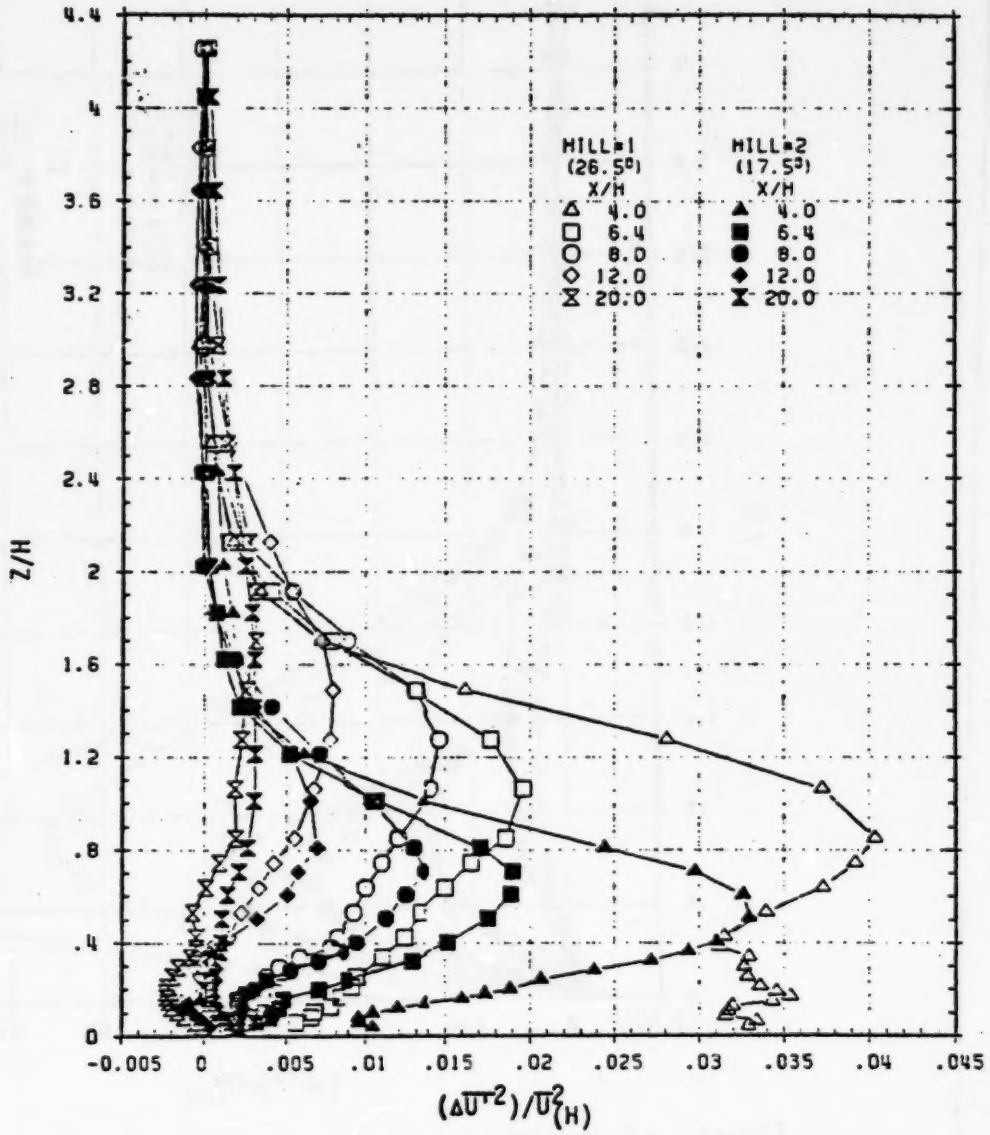

Figure 9. Distribution of perturbations in variances of longitudinal velocity ($\overline{u'^2}$)/$\overline{U}^2$(H) at various distances in the wakes of the hills.

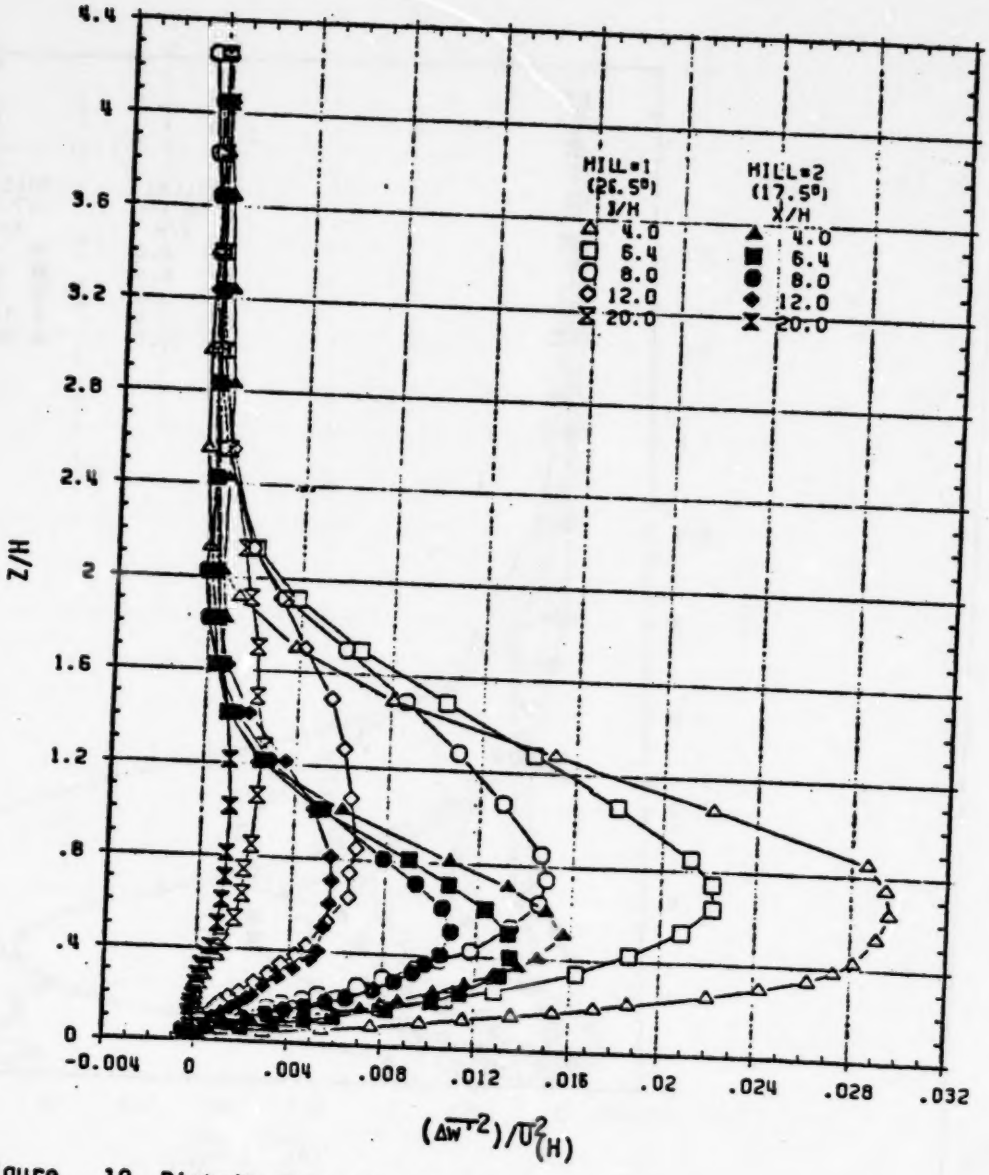

Figure 10 Distribution of perturbations in variances of vertical velocity $(\Delta\overline{w'^2})/\overline{U^2}(H)$ at various distances in the wakes of the hills.

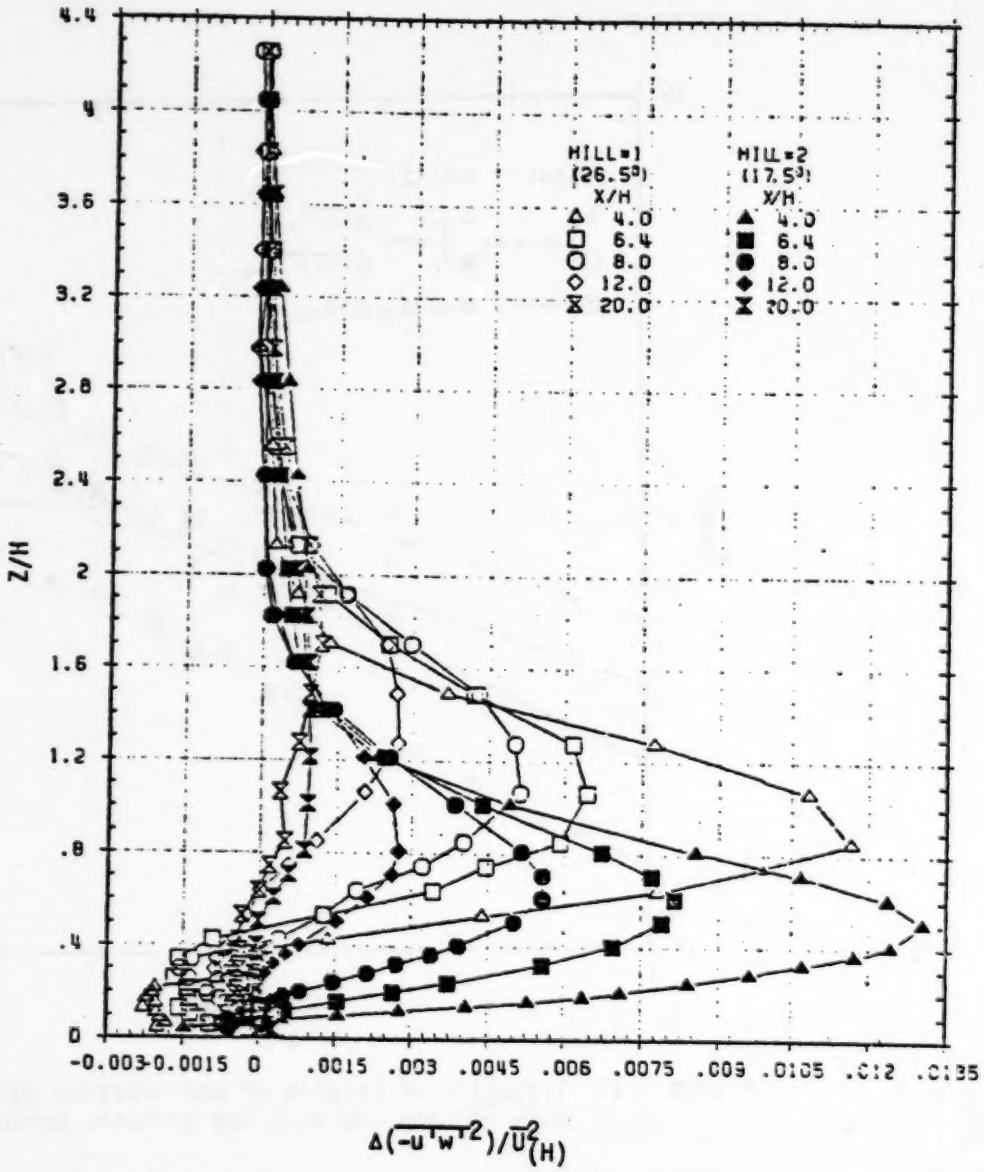

Figure 11 Perturbations in Reynold's stress $(\Delta(\overline{-u'w'}))/\overline{U^2}(H)$ at various distances in the wakes of the hills.

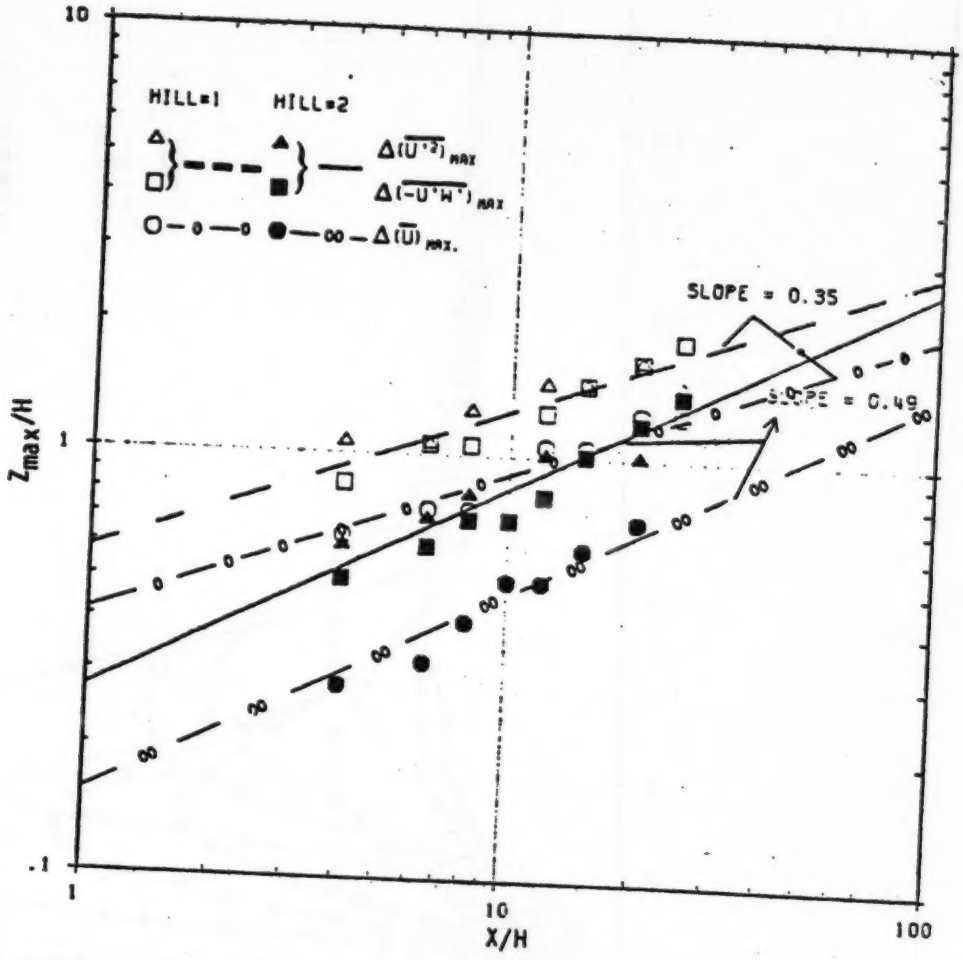

Figure 12 Variation of heights of perturbation maxima in $\Delta\overline{u'^2}$, $\Delta(\overline{-u'w'})$ and $-\Delta\overline{U}$ with the distance behind hills.

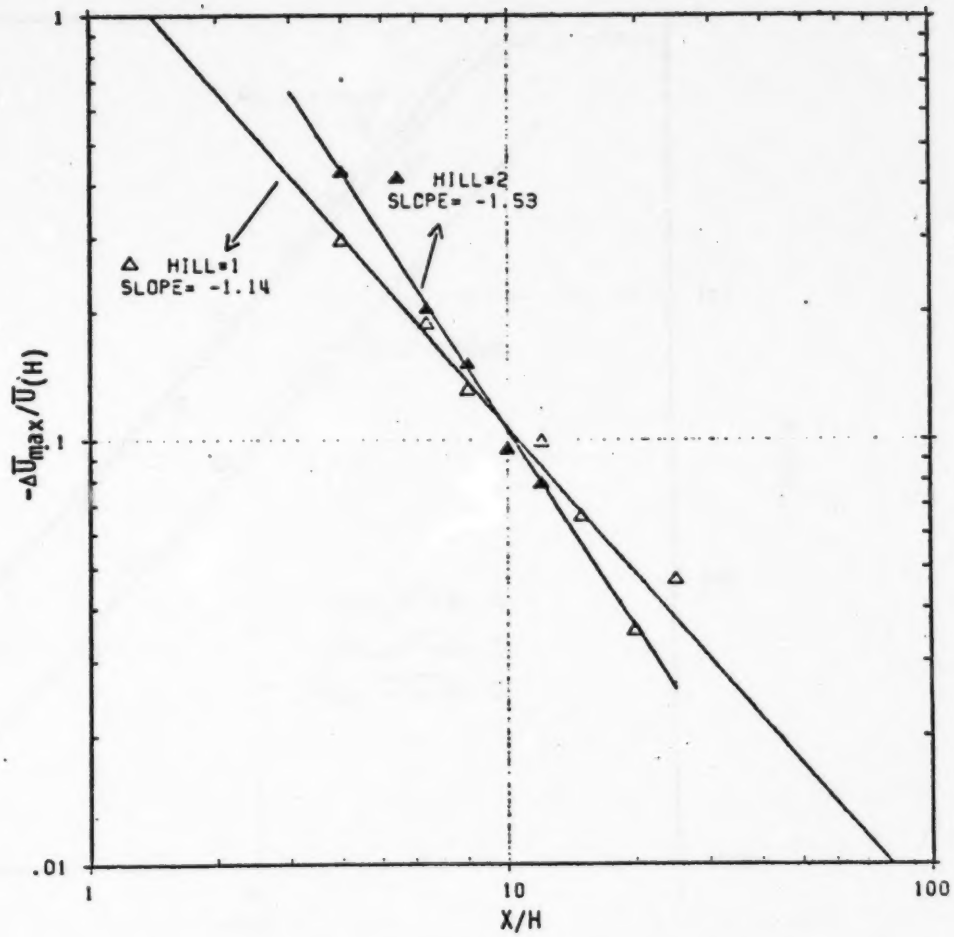

Figure 13 Variation of maximum mean velocity defect in the wake of the hills.

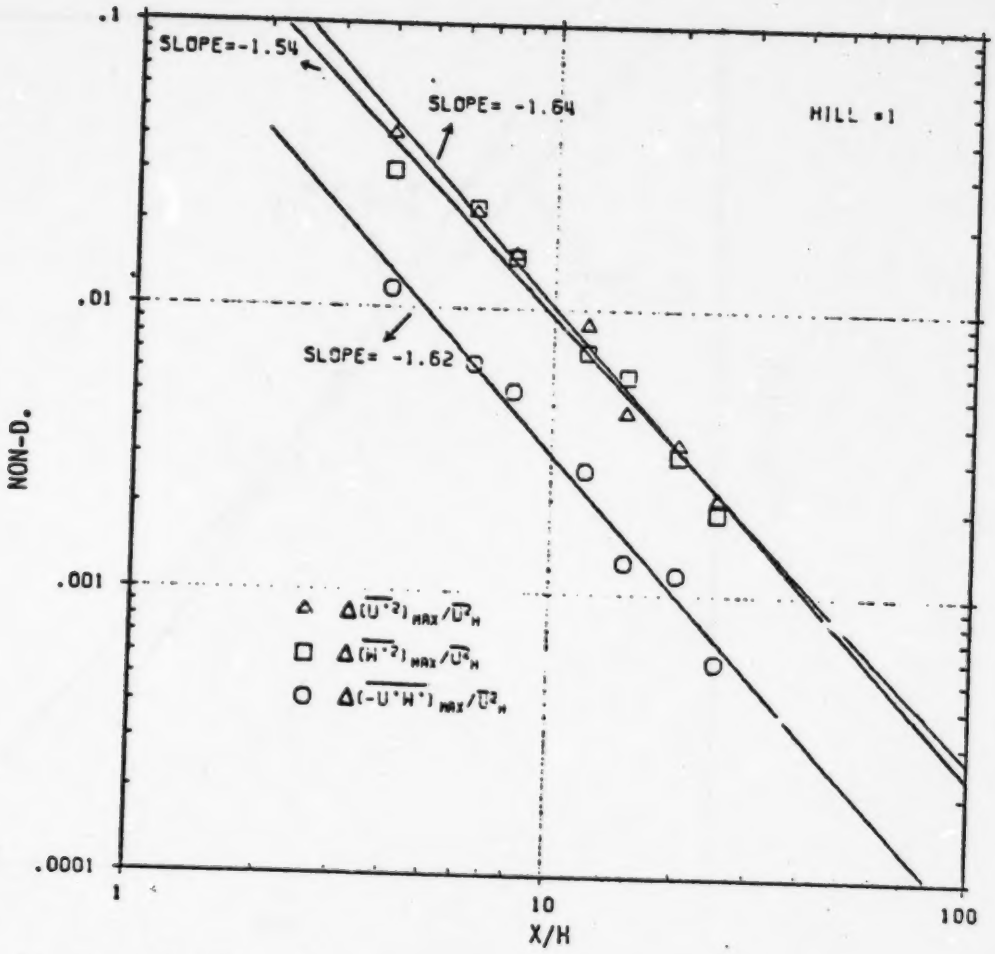

Figure 14a Variations in perturbation maxima of longitudinal and vertical velocity variances and Reynold's stresses in the wake of hill #1.

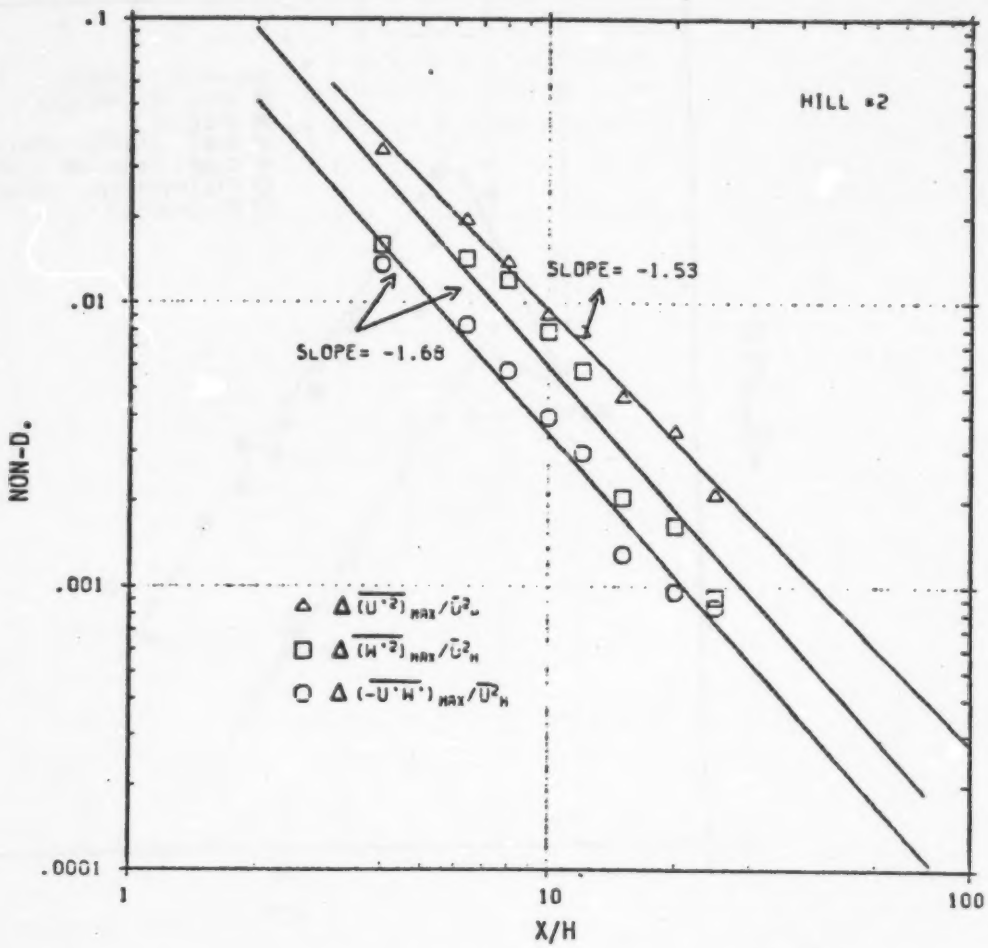

Figure 14b Variations in perturbation maxima of longitudinal and vertical velocity variances and Reynold's stresses in the wake of hill #2.

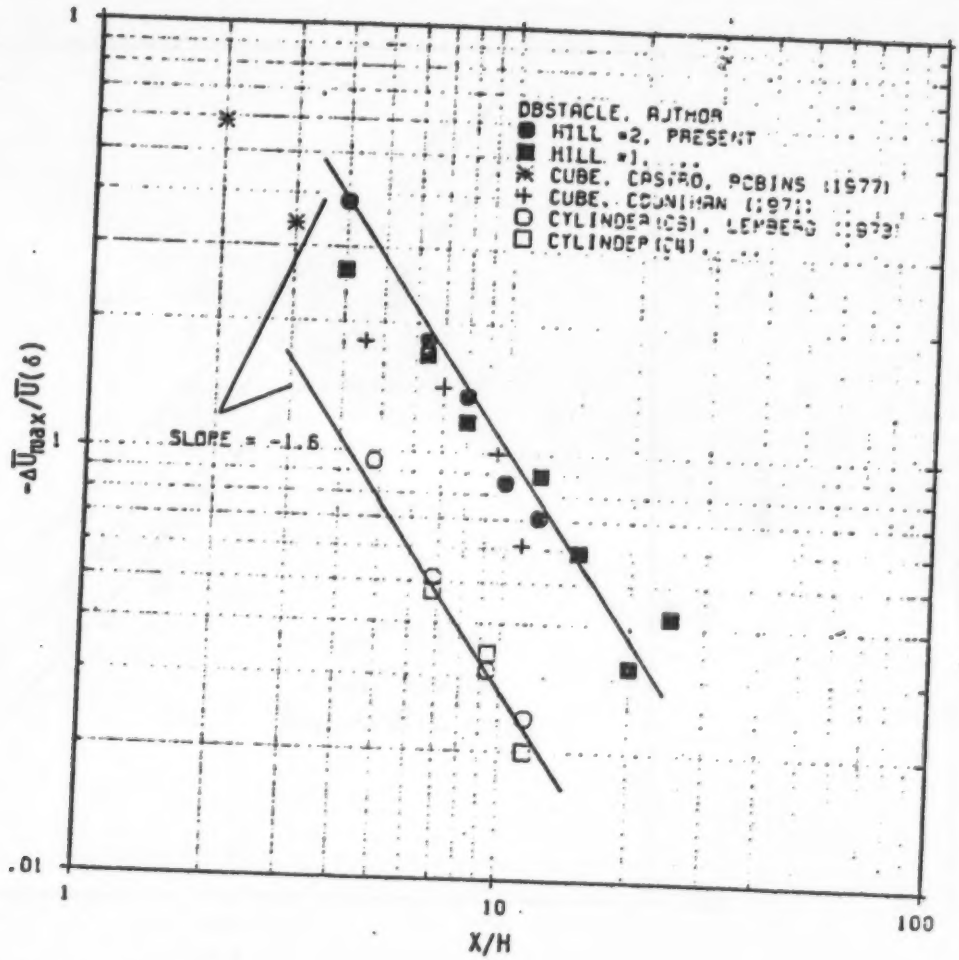

Figure 15. Comparison of variations of the maximum in mean velocity deficit the wakes of the various three-dimensional obstacles.

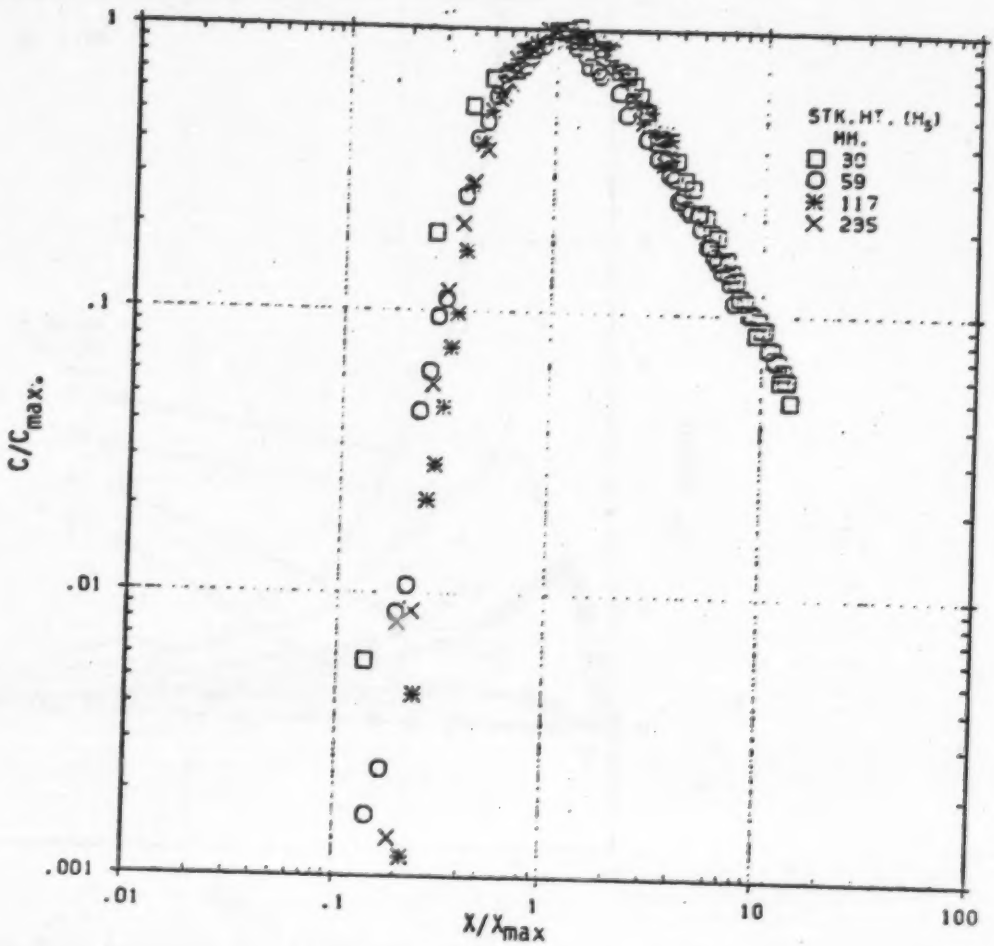

Fig. 16. Similarity representation of longitudinal glc profiles downwind of elevated sources in the undisturbed boundary layer.

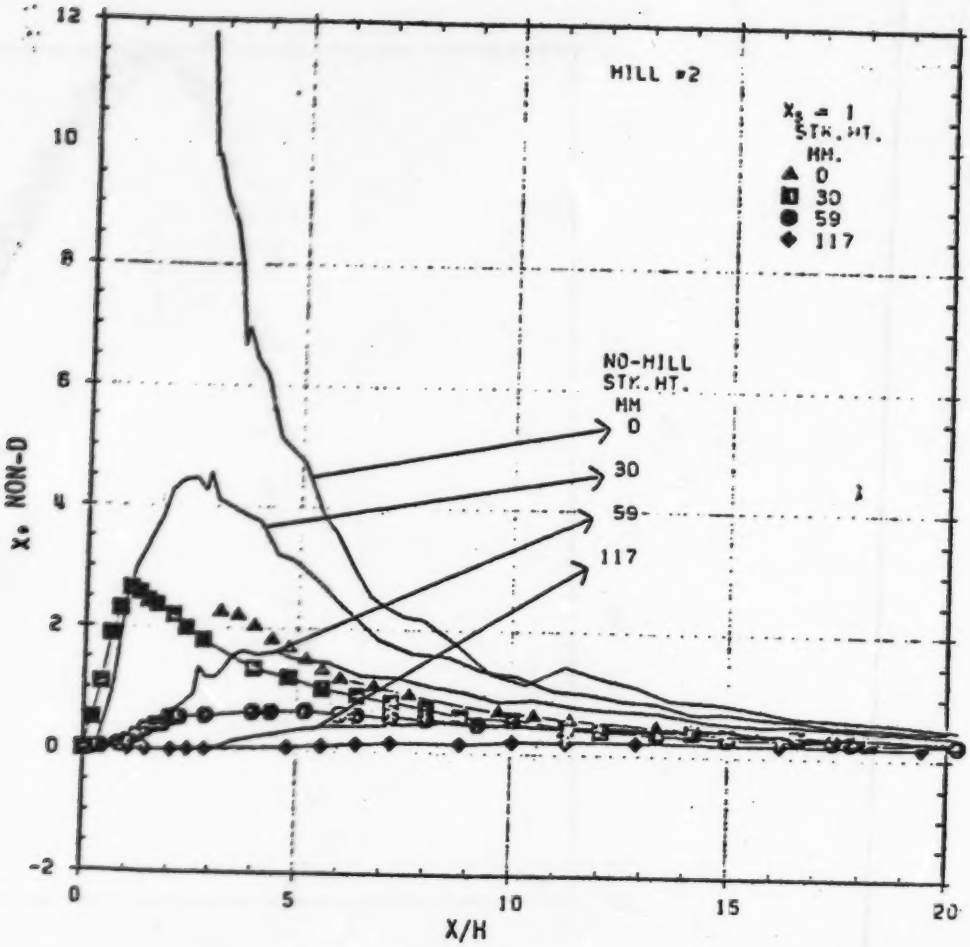

Fig. 17. Comparison of longitudinal glc profiles with and without the hill fo sources located at the hill top.

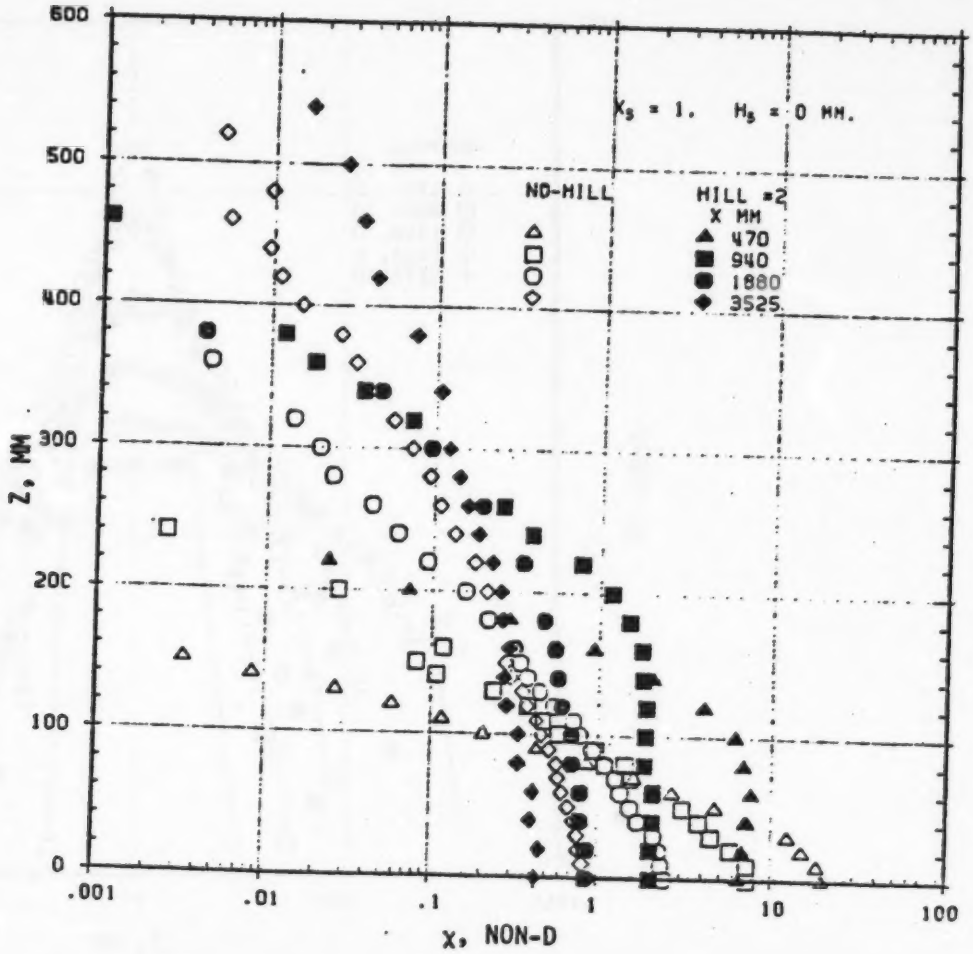

Figure 18. Vertical concentration profiles from a surface release at various downwind distances from the source. Open symbols represent undisturbed (no-hill) profiles. Source location: hill top.

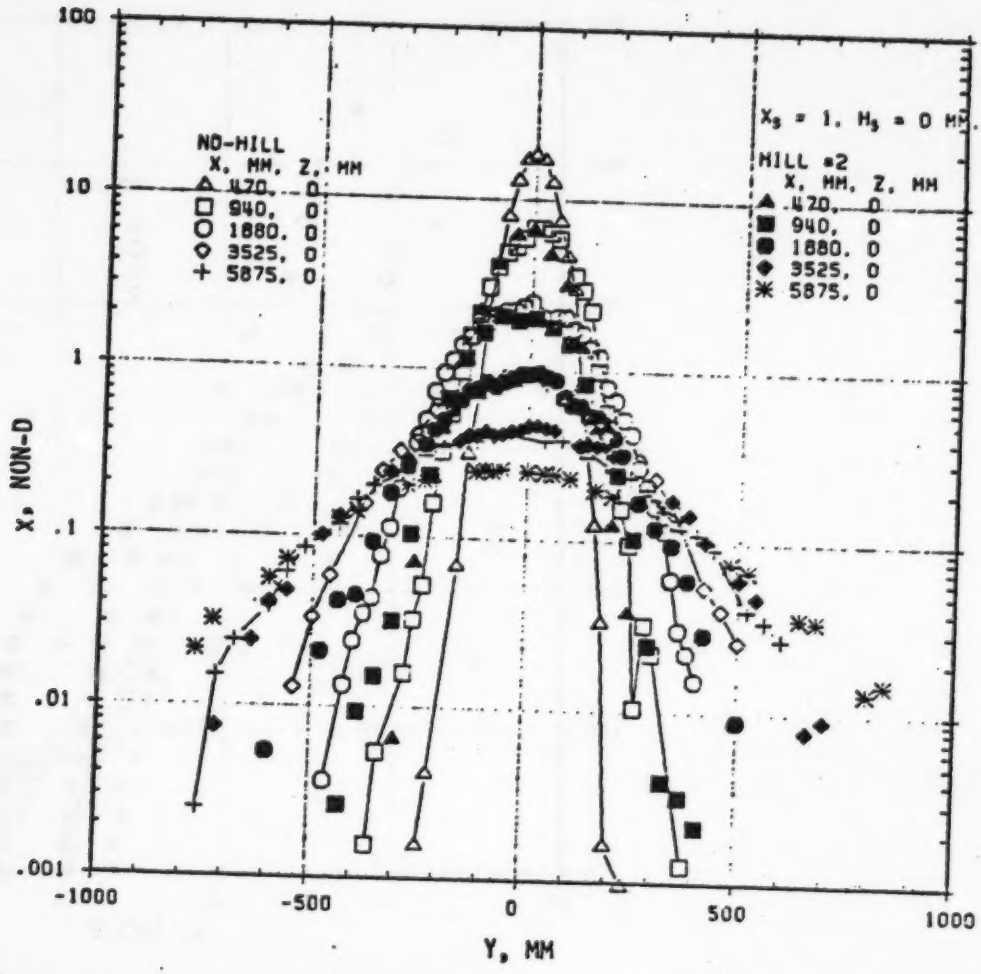

Figure 19.1 Comparison of lateral profiles between disturbed and undisturbed boundary layers. $H_s = 0$; $x_s = 1$ (hill top).

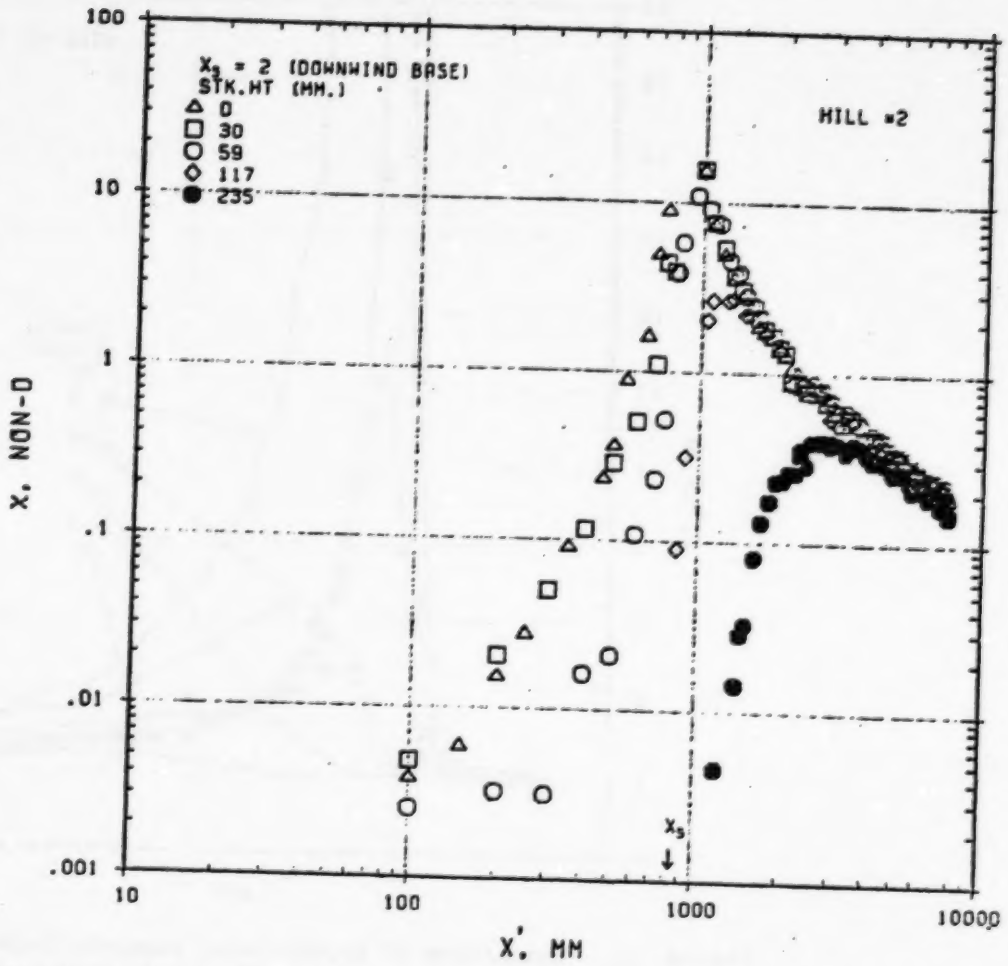

Figure 20. Surface longitudinal concentration profiles resulting from various stack heights located at the downwind base of hill #2.

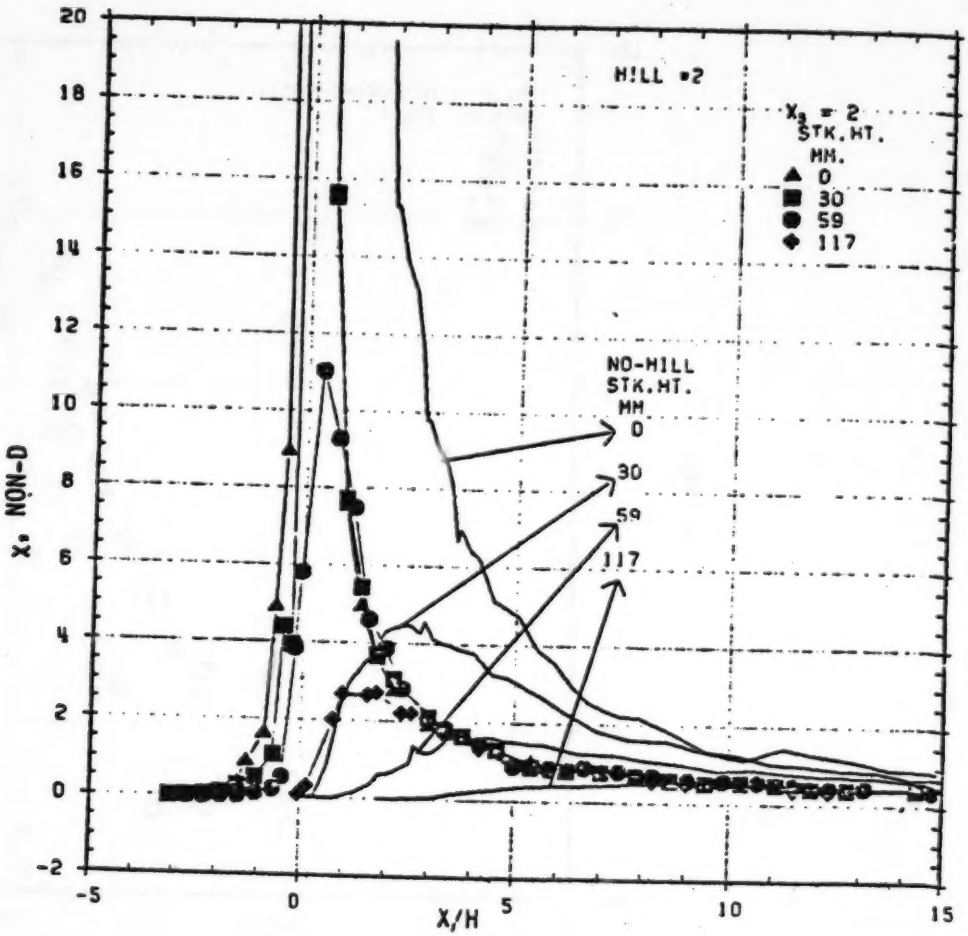

Figure 21. Comparison of ground-level concentration profiles with and without the hill. Source location: downwind base.

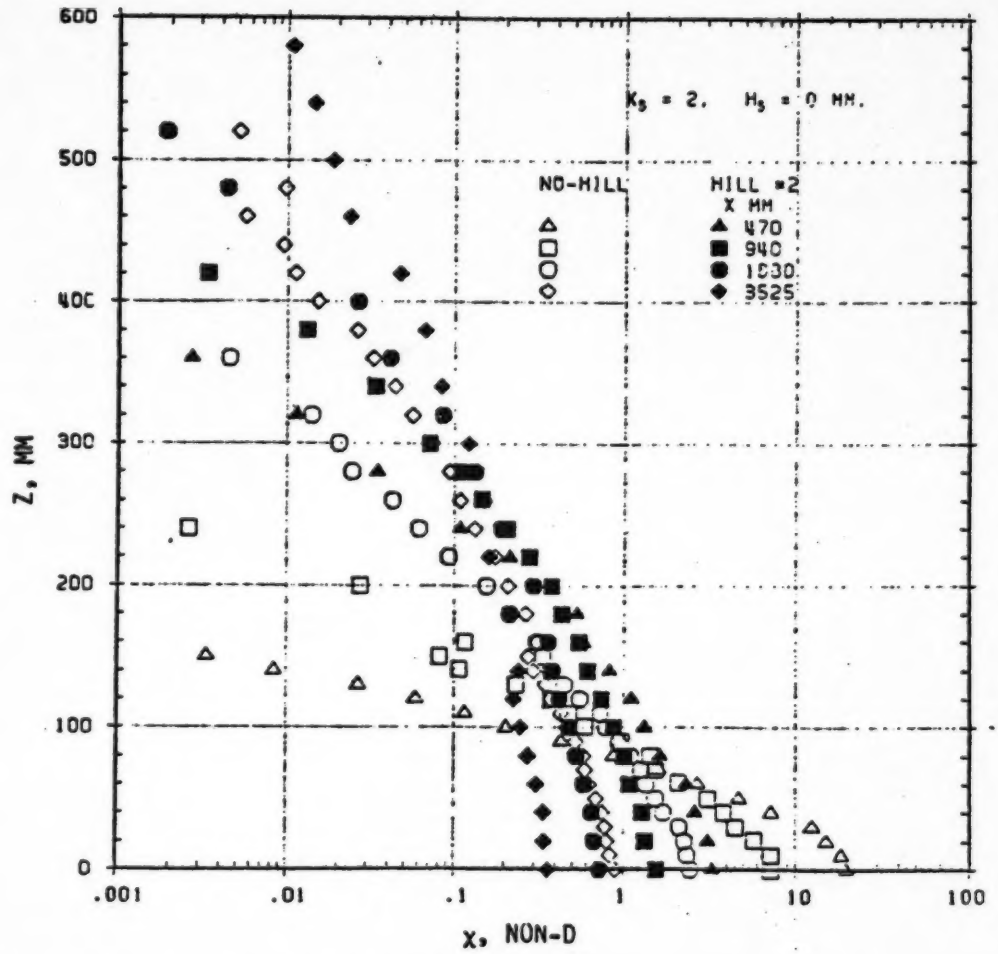

Figure 22. Vertical concentration profiles from a surface release at various downwind distances from the source. Open symbols represent undisturbed (no-hill) profiles. Source location: downwind base.